

**AN EXPERIMENTAL INVESTIGATION OF ICE-CONCRETE ADHESION
AND CORRESPONDING ABRASION**

By Titli Pramanik

A thesis submitted to the School of Graduate Studies in partial fulfilment of the
requirements for the degree of Master of Engineering

Faculty of Engineering and Applied Science
Memorial University of Newfoundland

February 2021

St. John's, Newfoundland and Labrador

Abstract

Concrete wear due to ice collision is a threat that marine structures in colder regions deal with. This phenomenon can cause damage to the structures, resulting in high maintenance costs. One damage mechanism may arise from ice sticking to the concrete under pressure and then damaging the concrete when the bond is broken by ice movement. The objective of this study is to experimentally measure adhesion strength between ice and concrete with various applied pressure and contact duration time under constant temperature for both dry and submerged conditions. A secondary objective is to measure the corresponding concrete abrasion arising from the ice bond breaking process. This thesis reviews previous laboratory work to identify the critical issues, including different areas with similar approaches. Significant parameters, contributing factors, and relevant design of test setups were reviewed from previous studies. Based on these factors, the rationale of the current study was developed, and the experiment was designed accordingly. A pilot experiment was designed to explore design factors for the main experiment. Considering these findings, a new apparatus was designed and the test setup was modified to conduct the experiment. The experiment was designed in a 7x7 square matrix format. The tests were conducted and a nonlinear relationship was obtained from the data set. Photographs were taken, and sample weights were measured before and after the tests to obtain the material loss for both ice and concrete samples. Statistical analysis was conducted with the collected data to obtain the impact of the independent variables on the test result. The observed trends were found to be statistically significant.

Acknowledgement

It was an amazing experience to pursue my master degree in civil engineering from Newfoundland. My childhood dream came true during this research journey. I would like to thank the Memorial University of Newfoundland and Kvaerner Canada Ltd for their financial support to this research project. My heartfelt thanks to my supervisors Dr. Stephen Bruneau and Dr. Bruce Colbourne, for their precious knowledge, guidance, and lessons during this entire journey. Besides the technical and scientific knowledge, they developed my scientific philosophy. This study would not have been possible without their support, encouragement, and scientific discussions, even during the pandemic. No words will be sufficient to describe their contributions to this research work.

My sincere thanks to Dr. Amgad Hussein and Dr. Assem Hassan for their technical advice and help. Our team members Ali Eed Abdel Hafez and Mohamed Zurgani helped me a lot for designing the concrete mix. Thanks to Ahmed Taha, Dr. Basem Hassan , Dr. Mohamed Karam, for their advice. Many thanks to Bart Westerveld, Bob Tulp, Nynke Nuss, Anne Barker, Yiran Liu, Mwaria Emmanuel Richmond, and my all colleagues. It was a fantastic experience to work with all of you.

A special thanks to Matthew Curtis, Craig Mitchell, David Snook, William Bidgood, Trevor Clark, and other laboratory technicians for sharing their technical knowledge and enthusiastic assistance during the experiment. I will always remember their uncountable assistances in the laboratory.

I would like to thank Dr. Rocky Taylor for his ice mechanics course; although I was an audit student, he helped me to grow my knowledge in ice mechanics. My cordial, thanks to Dr. Ashok Shaw, Dean of my undergraduate school, for his motivation and guidance in my academic career. I am thankful to my mentor Mr. Darrell Cole, for his professional and

philosophical advice in my career. Thanks to Ms. Vanessa Coish for the regular invitation to technical events and countless help with the official matters. Thanks to Ms. Kathryn Hong for arranging the technical events for industrial outreach. It was so nice to work with you.

This journey was not possible without my friends and family. Many thanks to my cousin Dr. Aakashneel Bhattacharya, my sister in law, Dr. Sanghamitra Sinha, and my friend Asmita and Juhi for their emotional support.

Endless thanks to my Ma and Baba (mom and dad) for their support, help, and advice. You both gave me the freedom to choose my own path, encourage me to pursue my dream, and had faith in me during the tough times.

Finally, thank you so much, Abhinaba, for being a husband, friend, advisor, and companion during my entire career journey since we met. You are the one who inspired me to be a researcher and helped me in all possible ways to come to Newfoundland and pursue my dreams. This thesis is for you.

Table of Contents

Abstract.....	ii
Acknowledgement.....	iii
List of Tables.....	v
List of Figures.....	ix
Chapter 1 Introduction	12
1.1 Background.....	12
1.2 Objective.....	13
1.3 Thesis Outline.....	14
Chapter 2 Literature Review	16
2.1 Friction and Sliding Abrasion Studies.....	16
2.2 Adfreeze and Pile Loading Studies	25
2.3 Other Considerations of Ice Adhesion and Abrasion	32
2.3.1 Ice Adhesion Theory.....	35
2.4 Summary of the State of the Art Regarding Ice Bonding and Concrete Wear.....	40
2.5 Rationale for this Study	40
Chapter 3 : Experiment Criteria, Design and Implementation.....	42
3.1 Design Criteria of Apparatus.....	42
3.1.1 Velocity –Loading Rate, Start- Stop, Adhesion.....	42
3.1.2 Applied Pressure	43
3.1.3 Dry and Submerged Tests.....	45
3.1.4 Ice Type	45
3.1.5 Concrete Type.....	46
3.1.6 Temperature	46

3.1.7 Measurement of Applied Pressure and Adfreeze Bond Strength	47
3.1.8 Measurement of Concrete Abrasion	47
3.1.9 Examination of Coarse Aggregate Rock Core and Cement Paste	48
3.1.10 Loading and Unloading.....	48
3.1.11 Summary of Design Criteria	48
3.2 Concept Design.....	49
Chapter 4 : Experiment and Analysis.....	53
4.1 Pilot Experiment	53
4.2 Surface Interaction.....	55
4.3 Sample Preparation.....	56
4.3.1 Ice Samples	56
4.3.2 Concrete Sample	60
4.3.3 Concrete Aggregate Sample	63
4.3.4 Mortar Sample	65
4.4 Instruments and Equipment.....	65
4.4.1 Lever Arm Apparatus	65
4.4.2 Mechanism and Load Calculation	68
4.4.3 Aluminium Clamp	68
4.4.4 Box for Submerged Experiment	69
4.4.5 Scissor Jack and Drill.....	70
4.5 Dependent and Independent Variables	72
4.6 Design of Experiment.....	73
4.7 Results	74
4.8 Analysis	79
4.8.1 Data Validation	86
4.9 Material Loss and Findings	87
4.9.1 Concrete Material Loss	87

4.9.2 Ice Indentation and Loss of Ice Surface.....	88
4.9.3 Ice Adhesion over Aggregate.....	89
4.10 Submerged Experiment	90
Chapter 5 Discussion and Conclusions	94
5.1 Experimental Findings and Discussion	94
5.1.1 Contact Persistence	95
5.1.2 Ice Concrete Interface	95
5.1.3 Concrete Abrasion	95
5.1.4 Adhesion to Aggregate	96
5.1 Summary.....	96
Chapter 6 Limitations and Recommendations	98
6.1.1 Ranges of Independent Variables	98
6.1.2 Controlled Environment and Equipment	98
6.1.3 Surface Roughness Measurement and Microscopic Analysis	99
6.1.4 Compressive test of Rock Samples.....	99
6.2 Recommendation for Future Research	99
6.2.1 Items that could not be completed	99
6.2.2 Inclusion of Other Independent Variables	100
6.2.3 Variation of Concrete Mix Design.....	100
6.2.4 Full Scale and Long term Experiment	101
6.2.5 Statistical Analysis.....	101
References	103

List of Tables

Table 3.1: Design Requirement and Criteria.....	49
Table 4.1: Concrete mix design for 1 m ³	61
Table 4.2: Result of Compressive Test of Concrete after 14 and 28 Days).....	62
Table 4.3: Parameters of Experiment.....	73
Table 4.4: Experiment Matrix	74
Table 4.5: All trials: Adhesion Strength (N) between ice and concrete with varying force and duration under constant temperature (-1° C).....	76
Table 4.6: Average Adhesion Strength (kPa) between ice and concrete at varying pressure and duration under constant temperature (-1° C).....	77
Table 4.7: Multiple Regression Analysis of Collected Data.....	80
Table 4.8: Contact Persistence and Corresponding Adhesion Strength.....	81
Table 4.9: Statistical Analysis of Contact Persistence and Adhesion Strength	82
Table 4.10: Comparison between Regression Output of Original Data and Contact Persistence	82
Table 4.11: Comparison of Theoretical and Practical Output.....	87

List of Figures

Figure 1.1: Flowchart of Thesis Content.....	15
Figure 2.1. Laboratory Test Setup (Saeki et al., 1984)	17
Figure 2.2: Mechanism of Laboratory Experiment conducted by H. Saeki, 1986.....	18
Figure 2.3: Laboratory Test Setup (Itoh et al., 1988).....	19
Figure 2.4: Mechanism of laboratory Test Setup by Y. Itoh, 1988.....	20
Figure 2.5: Concrete Specimen and Traverse Line (Itoh et al., 1988)	20
Figure 2.6: Laboratory Abrasion Machine (Huovinen, 1990)	22
Figure 2.7: Experimental Setup (Greaker, 2014)	23
Figure 2.8: Experimental Setup (Tijssen et al., 2015)	24
Figure 2.9: Experimental setup of Pull out test (Nakazawa et al., 1988).....	27
Figure 2.10: Experimental Setup (Terahima et al., 2006).....	28
Figure 2.11: Cracks Formation During Pull-Up Test (Terahima et al., 2006).....	28
Figure 2.12: Mechanism of Pull out Experiment (Saeki, 2011).....	29
Figure 2.13: Experimental Setup to Test Adfreeze Bond (Saeki, 2011).....	30
Figure 2.14: Surface Roughness Effect on Adfreeze Bond Strength of Various Materials at -5°C Temperature (Saeki 2011).....	31
Figure 2.15: Effect Causing Damages to Concrete in Sea Ice (Huovinen, 1990).....	33
Figure 2.16: Schematic Diagram of Concrete Abrasion Mechanism (Jacobsen et al., 2015)..	35
Figure 2.17: Water Drop on Solid Surface and definition of Contact angle (Makkonen, 2012)	36
Figure 2.18: Simplified Illustration of Ice-Concrete Interface for a Vertical Concrete Structure (Jacobsen et al., 2015)	38
Figure 3.1: Mechanism of Ice adhesion to a Material surface (Saeki, 2011).....	44
Figure 3.2: Basic Mechanism of Experimental Setup.....	51

Figure 4.1: Pilot Experimental Setup	54
Figure 4.2: Surface Indentation	55
Figure 4.3: Schematic Diagram of Ice Preparation (Bruneau et al., 2013)	57
Figure 4.4: Preparation of Ice Sample	58
Figure 4.5: Dimension of Ice Sample	59
Figure 4.6: Thin Section of Ice Sample	59
Figure 4.7: Aluminium Plate on the Ice sample to Minimize the Displacement	60
Figure 4.8: Concrete Sample;	62
Figure 4.9: Compressive Strength Testing	63
Figure 4.10: Aggregate Samples	64
Figure 4.11: Procedure of Cutting Rock Sample	64
Figure 4.12: Aggregate Testing Samples	65
Figure 4.13: Diagram of Lever Arm	66
Figure 4.14: Experimental Setup	67
Figure 4.15: Aluminium Holder of Concrete Sample	69
Figure 4.16: Metal Box for Submerged Test	70
Figure 4.17: Mechanism of Scissor Jack	71
Figure 4.18: Ice-Concrete Adhesion Pressure versus Contact Duration at Various Normal Stresses	79
Figure 4.19: Normal Probability Plot of Multiple Regression Analysis	83
Figure 4.20: Normal Probability Plot of Linear Regression Analysis	83
Figure 4.21: Fitted Curve of Adhesion Strength under 112.49 kPa Contact Pressure	84
Figure 4.22: Fitted Curve of Adhesion Strength under 426.7 kPa Contact Pressure	84
Figure 4.23: Fitted Curve of Adhesion Strength under 826 kPa Contact Pressure	85
Figure 4.24: Fitted Curve of Adhesion Strength under Varying Pressure and Duration	85

Figure 4.25: Contact Persistence vs Adhesion Strength	86
Figure 4.26: Surface Material Loss of Concrete Sample after Series of Experiments.....	88
Figure 4.27: Ice Surface before and after the Experiment with Abraded Concrete Particles ..	89
Figure 4.28: Ice Piece Sticking to the Concrete Surface after the Experiment.....	90
Figure 4.29: Mechanism of Submerged Experiment	91
Figure 4.30: Ice Piece Sticking on to the Concrete Surface after the Submerged Test	92
Figure 6.1: Research Objective and Future Opportunities.....	102

Chapter 1 Introduction

1.1 Background

Ice interaction is a significant factor that marine structures in colder region often have to deal with. Moving sea or river ice may cause concrete abrasion due to continuous or intermittent ice interaction with the waterline area of structures such as dams, piers, or offshore structures. This continual or seasonal ice induced wear results in gradual material loss and concrete degradation over long periods and can result in serious damage to the structures. The degree of ice induced wear is highly dependent on the characteristics of the ice, the properties of the concrete, and the nature of the interaction. Parameters such as the contact pressure and surface roughness have been shown to be important.

One possible physical mechanism of abrasion is the bonding of ice to the concrete, which may result in a material loss when the bond is broken. This scenario would occur in cases where ice is pressed against a structure for a period of time and then is forced to move by changing environmental conditions such as wind or tide. This mode of abrasion has not been extensively studied as most previous work has only considered sliding abrasion where ice and concrete interact in a continuous relative motion mode.

This study explores the adhesion of ice to concrete under varying pressure and duration. The purpose is to experimentally determine the strength of the ice-concrete bond as a function of the interface pressure and the duration of contact. Based on the data collected, a relationship is developed and normalized, which can be used to explore the ice bonding properties of different concrete mixtures to improve concrete abrasion or bonding resistance for harsh environments by minimizing the bonding strength of concrete mixtures.

1.2 Objective

The research objective of this project is to better understand and develop a relationship for the strength of ice-concrete bonding as a function of contact pressure and the duration of contact. A secondary objective is to determine the amount and nature of material lost from the concrete when ice-concrete bonds are broken. This is an initial study of ice-concrete bonding, and thus, the number of parameters has been limited to simplify the experiments and make the results as unambiguous as possible. The bond pressure and breakage is limited to the compressive-tensile direction. A single type of concrete mix is used. The temperature is held at an approximately constant value of -1° to -2°C .

This research is an experimental study at a laboratory scale with purpose-designed apparatus and procedures that provide a more simplified approach than previous studies in terms of the nature of the bond and release interaction. The independent variables are contact pressure and contact duration, and the dependent variable is bond strength with a secondary effort to measure material loss.

Prior to conducting the experimental work, a review of the prior work in ice friction, wear and adhesion, and in particular interaction with concrete was conducted to provide an overview of current knowledge and to indicate where this study would be best directed. The review of state of the art supports the experimental approach and provided guidance on the experiments and parameters.

Following the review, the experimental procedures, the concept of the basic experimental mechanism, and parameters to be included in the experimental matrix were developed into an experimental plan. Some pilot experiments were initially conducted to explore concrete wear due to ice adhesion, and the practicalities of the proposed experiment. These pilot experiments led to some further modification of the experimental setup and provided some

criteria for the initial values of contact pressure, temperature and rates of force application, particularly for breaking the bond. Later the experimental plans were expanded to perform both dry and submerged tests to replicate real-life conditions.

1.3 Thesis Outline

Figure 1.11 illustrates the outline of this thesis with a flowchart to describe the major topics in the document. This study is described in five chapters. The first chapter provides the background, including the rationale for this work. The next chapter reviews the prior work in ice-concrete interaction with an emphasis on bonding, friction, and wear. Some identified gaps in the literature on bonding and wear lead to the current study. The third chapter describes the design of the experimental apparatus and the development of the experimental plan. The fourth chapter describes the conduct of the experiments and the collection and analysis of the data. A number of analysis methods are explored, and features of the collected data are discussed with a view towards developing relationships that can be extrapolated to real-life cases. The final chapter provides a discussion of the work, including conclusions, and some suggestions and recommendations for further work beyond this study.

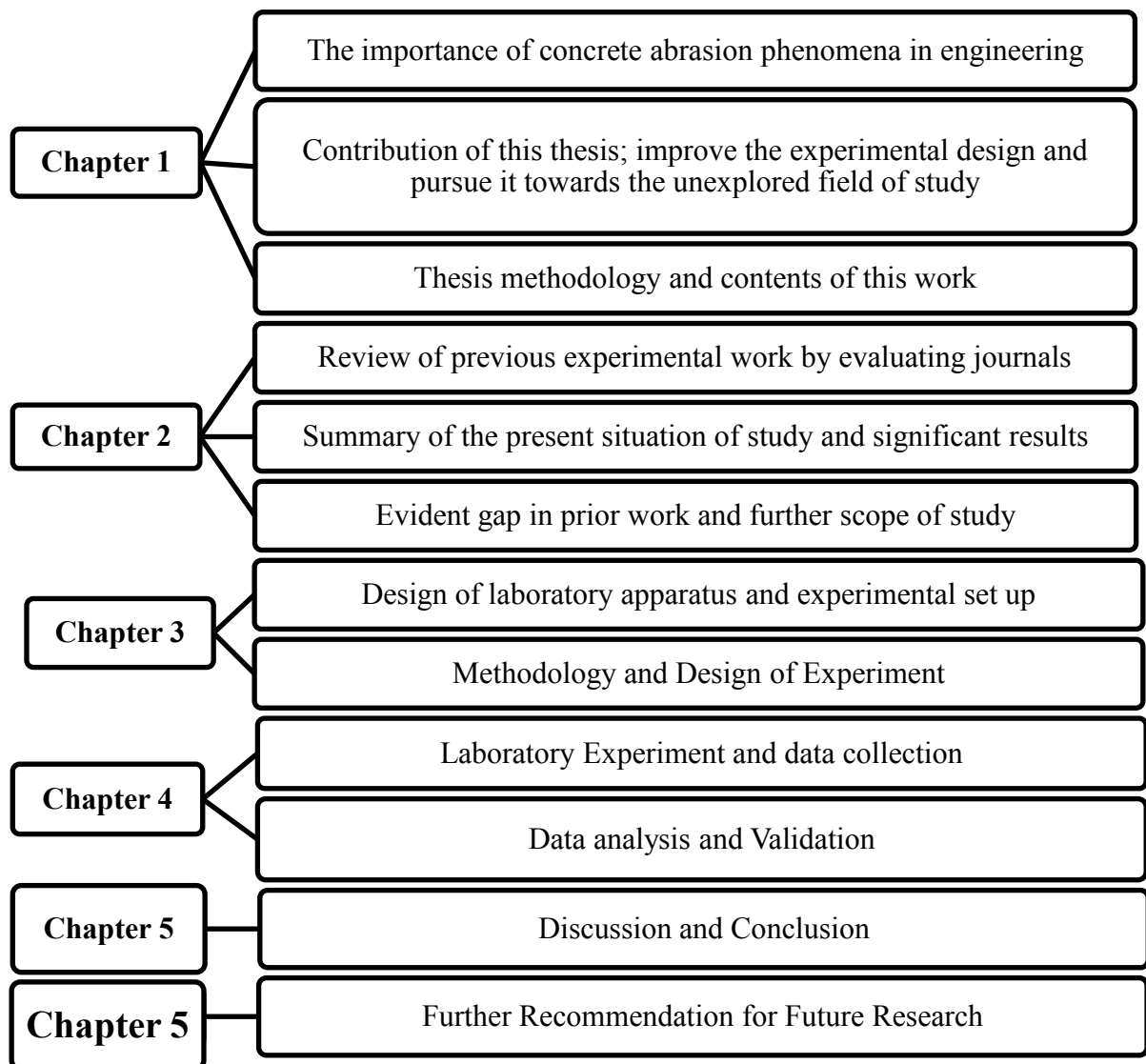


Figure 1.1: Flowchart of Thesis Content

Chapter 2 Literature Review

This chapter provides a review of previous studies covering ice interaction with concrete leading to bonding or concrete abrasion. Many of these previous studies are in the form of ice-concrete friction studies. The purposes of this review are to understand the previous scientific findings, assess previous methodologies, and inform the current study. In colder regions, ice loading and ice interaction are considered important factors for marine concrete structures such as bridge and light piers, dams, and wharves. Continuous or intermittent ice collision or relative motion causes material loss from the concrete surface. This action may reduce the structures' life span, increase maintenance costs or result in serious erosion damage over the life of the structure (Saeki, 2011).

2.1 Friction and Sliding Abrasion Studies

Several previous ice friction studies have been conducted with different test specimens to obtain the effect of parameters such as temperature, surface roughness, seawater etc. H. Saeki observed that ice shear strength increases with decreasing temperature (Saeki et al., 1984), (Hiroshi Saeki et al., 1985), (Saeki et al., 1985). Kinetic friction coefficients between sea ice and plastic, coating, and different metals were measured using normal stress up to 0.23 MPa (Gu et al., 1998). It was observed that the ice friction coefficients for most of the test materials vary a bit with normal stress. also documented that, with increasing velocity ranges from 5-25 cm/s, the kinetic friction coefficient decreases or changes a bit. Test results are also shown to vary with the experimental setup, Oksanen et al. (1980) has a similar observation of changes in friction coefficient under the relative velocity of 50-300 cm/s when the ice temperature was less than -5° C.

Another experimental study (Saeki et al., 1984) explores changes of friction coefficient under variations in temperature and other parameters (Figure 2.1). This sliding friction test was

conducted with sea ice and several offshore construction materials with different surface roughness, including concrete, under variable temperature and relative velocity for both dry and submerged cases. The experiment was designed to determine the effect of parameters such as relative velocity, contact area, temperature, submerged and dry conditions, sea ice growth direction, normal stress, and surface roughness. Although the study used the idea of friction coefficient, the variability of the coefficient as a function of the above parameters was noted. This is contrary to the idea of a conventional friction coefficient that is independent of velocity, normal force or pressure.

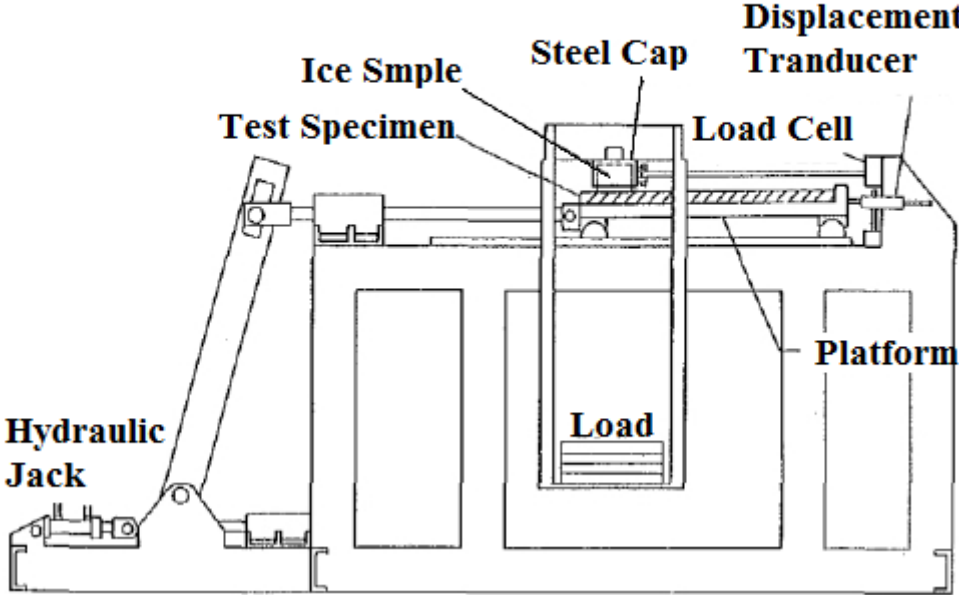


Figure 2.1. Laboratory Test Setup (Saeki et al., 1984)

The experiment was conducted using a horizontal moving platform connected to a hydraulic jack where an ice sample was placed over the construction material samples. The ice sample remained fixed during the test, and the construction material samples were moved. Ice temperature was the same as the air temperature during the experiment. A steel cap was used to keep the ice in place, and weights were placed on top of the steel cap to create a constant vertical loading on the ice. The hydraulic jack controlled the velocity of the material samples.

The horizontal velocity was applied 10 seconds after applying the vertical load. To measure the relative velocity, a displacement transducer was attached to the test platform. The friction force was recorded using a load cell attached to the steel cap used for holding the ice. The applied normal loading was calculated as the summation of the applied weight and the steel cap weight. Figure 2.2 illustrates the mechanism of this experiment.

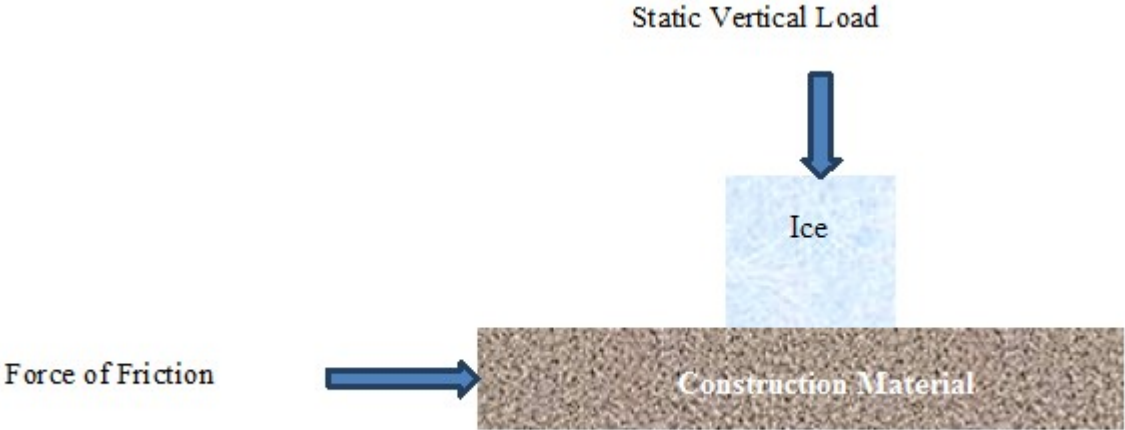


Figure 2.2: Mechanism of Laboratory Experiment conducted by H. Saeki, 1986

It was observed that the friction coefficient depends on temperature, surface roughness, and relative velocity. The friction coefficient increases with decreasing temperature, like shear strength, whereas kinetic friction was found to decrease with increasing normal stress. As kinetic friction strongly depends on the surface roughness, the test specimen surfaces were smoothed to cover the maximum surface area and avoid differences associated with roughness.

Another experimental study measured concrete abrasion due to sea ice (Itoh et al., 1988). This project modified the earlier experimental apparatus of H. Saeki and conducted tests between sea ice and three different concrete mixes. In this study, it was noted that the apparatus

requires variable contact pressure, relative velocity, and the ability to measure static and kinetic friction in order to understand ice friction better.

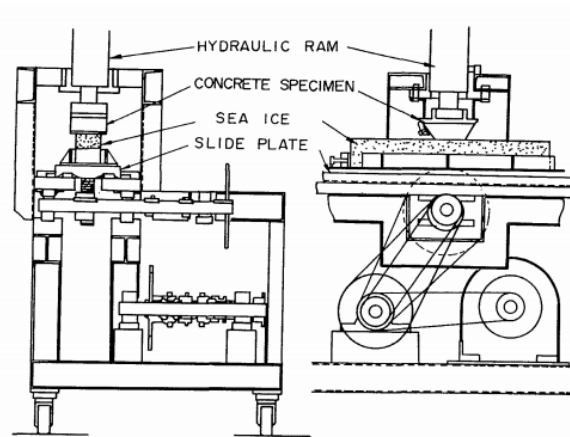


Figure 2.3: Laboratory Test Setup (Itoh et al., 1988)

Figure 2.3 shows the apparatus. Itoh's experiment was conducted by placing the concrete specimen over an ice block where the margins of the ice and concrete samples were not in contact, as the widths of the concrete specimen and the ice block were 10 and 8 cm respectively. The margins were used as a datum for measuring the concrete abrasion after the test. The sea ice on the sliding plate has dimensions of 70x8 cm with a thickness of 5 or 10 cm. The concrete sample was placed over the ice sample, and varying contact pressure was applied with a hydraulic ram. Reciprocating motion in the sliding plate was used to measure both static and kinetic ice friction against the concrete sample. The methodology of this experiment is illustrated in Figure 2.4.

The test was stopped when the ice specimen was significantly abraded, and then resumed with a new ice specimen. The concrete surface was measured before and it was measured after the experiment through the five traverse lines (Figure 2.5); the air temperature of the test room was constant, and the ice specimen temperature was collected at each rest during the experiment. This test setup had the provision to remove abraded ice from the interface with an

air blower; the air temperature from the blower was the same as the ice sample, so the air also helped reduce the frictional heat from the ice block surface.

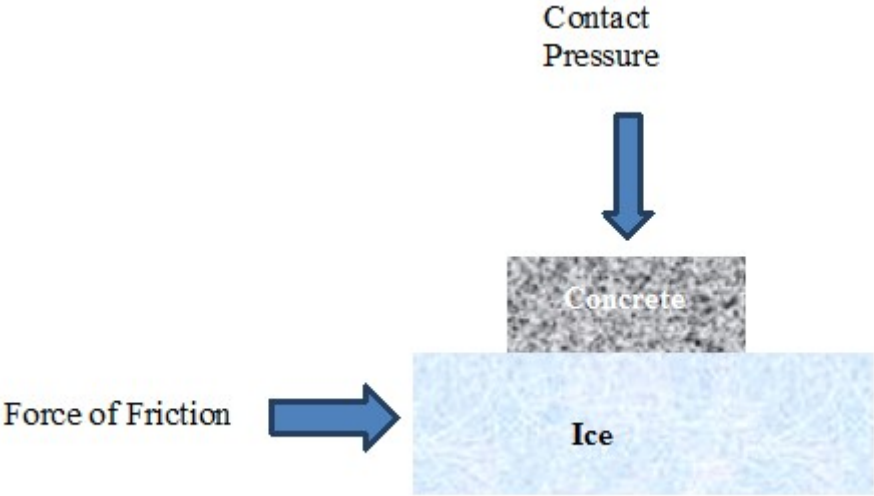


Figure 2.4: Mechanism of laboratory Test Setup by Y. Itoh, 1988

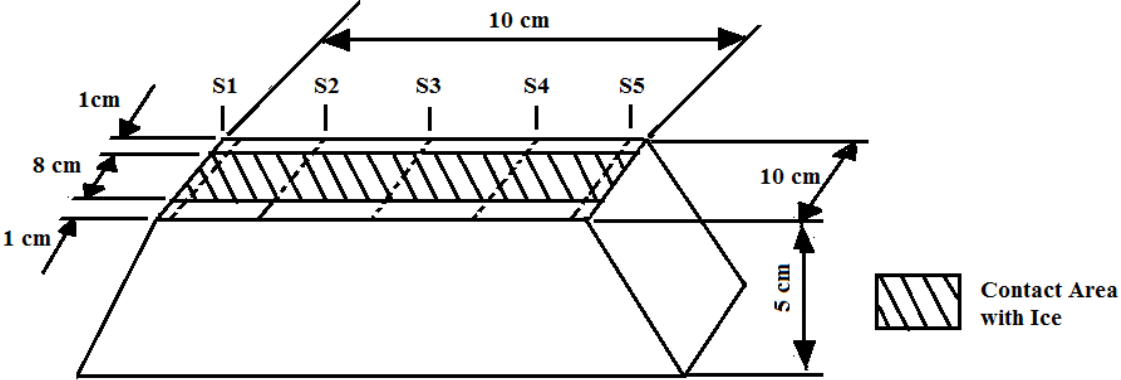


Figure 2.5: Concrete Specimen and Traverse Line (Itoh et al., 1988)

This study used various ice and concrete samples. Ice specimens had salinity of 35 ‰ with density in the range of 0.90 to 0.92 g/cm³. Concrete strength, durability and abrasion are highly dependent on the aggregate and surface treatment. Polyurethane resin lining, polymer impregnation, and resin mortar lining were applied as surface treatments and the concrete sample mixes were designed with different aggregates including normal aggregate, lightweight coarse aggregate and normal fine aggregate, lightweight fine and coarse aggregate

, lightweight fine and coarse aggregate, which have corresponding strengths of 350, 568 and 700 kgf/cm respectively. Relative velocity, (1, 5, 203 cm/sec), temperature (-5, -10, -20°C) and contact pressure (5, 10, 15, 20, 30 kgf/cm²) were variables in the experiment.

The test results showed the basic wear mechanism and the effects of the different parameters on the concrete abrasion. Regardless of the compressive strength and aggregate type of concrete, the uncoated concrete degradation process was divided into three steps – surface region, transition region, and stable region. The cement paste degraded relatively quickly in the surface region and exposure of the coarse aggregate occurred in the transition region, which finally leads to coarse aggregate abrasion in the stable region- where wear rate is much slower but causes serious damage to the structure.

The concrete abrasion is mostly dependent on the contact pressure and temperature.

As a larger concrete wear rate was found with the ice temperature below -10°C, a possibility of salt precipitation was considered below -8°C, which may induce the higher concrete wear rate. The concrete abrasion was found to be linearly increasing for each ice temperature when the contact pressure increases. When the experiment was conducted at -5°C and -10°C and the contact pressure exceeded 20 kgf/cm, the test could not be completed as the ice block started disintegrating because the contact pressure was close to the crushing strength of the ice block. The effect of relative velocity, compressive strength, and aggregate type of concrete were all found to have a comparatively mild influence on the concrete wear rate.

Based on these findings, polyurethane resin lining or resin mortar lining was suggested as a surface treatment to reduce concrete abrasion. This lining reduces the friction between the structure and the sea ice, whereas mortar improvement treatments like steel fiber reinforcement or polymer impregnation were found to be ineffective as wear reducing surface treatments.

Huovinen (1990) conducted experiments where abrasion resistant concrete mixes were subjected to multiple freeze thaw cycle before abrasion testing, as the fine concrete particles are abraded due to obtruded aggregate stones, the ice force was measured against those aggregate stones in the laboratory (Figure 2.6). Additional field experiments were also conducted by placing the concrete specimen on the bow of an ice breaker at the waterline level to measure concrete wear rate in sea water.

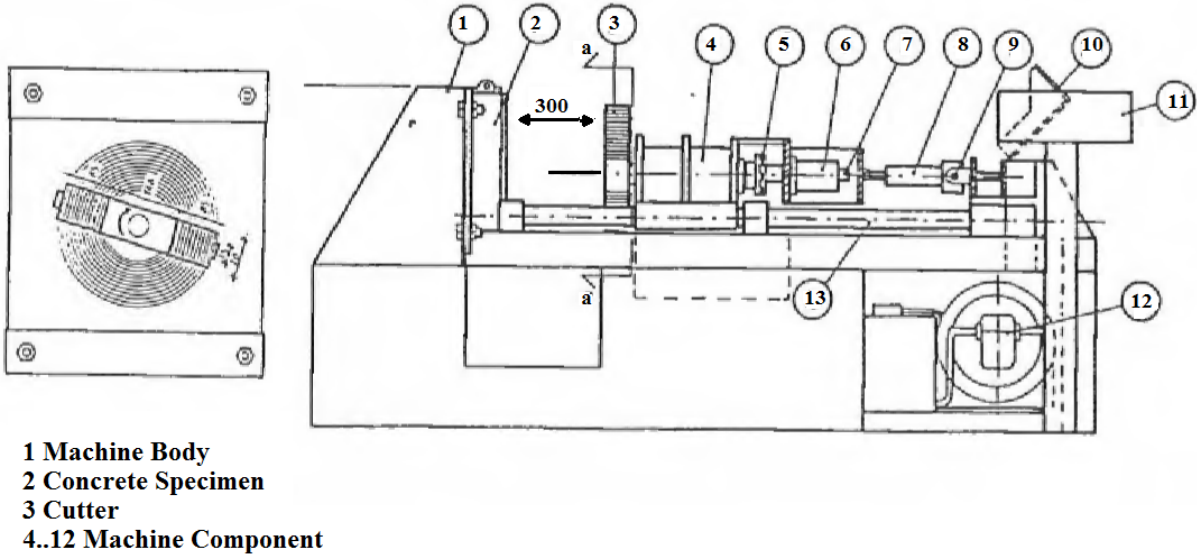


Figure 2.6: Laboratory Abrasion Machine (Huovinen, 1990)

Huovinen also explained the mechanism of concrete structure abrasion due to sea ice interaction. The effect of concrete abrasion can be physical, chemical, or mechanical depending on the ice loading effect. The pressure of freezing water and shrinkage of concrete due to temperature fluctuation can cause cracks in the structure; thus moisture and salt can penetrate the concrete and cause physical damage. Mechanical abrasion damage is caused by sea ice collisions against the structure. As a result, the finer concrete materials are worn off, and the aggregate stones are exposed leading to more serious mechanical damage.

Greaker (2014) designed a sliding experiment between 5 different ice samples and concrete where the concrete samples were cast 5 years prior to the experiment, stored in a moist condition for the first two years and then exposed to the air. The average compressive strength was found 51 MPa. 12 concrete sample surfaces were flattened while 3 had cast surfaces and surface roughness was measured with a digital indicator before and after each test. Ice samples were frozen at different temperatures and processed from either; tap water, the combination of slush and tap water, carbonated water or drilled from a block of unidirectional ice. The sliding distance was 500m, and the mean abrasion was collected as the ratio of mean abrasion depth and effective sliding distance (Figure 2.7). This study concluded that the concrete wear rate increases when the surface is rough.

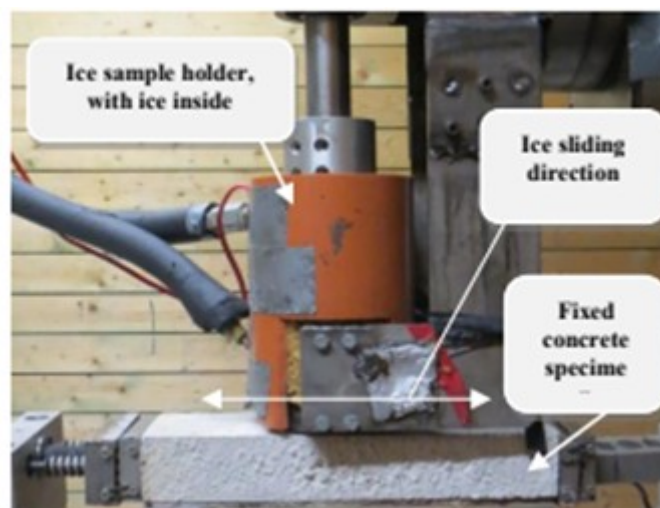


Figure 2.7: Experimental Setup (Greaker, 2014)

Tijssen, Bruneau, and Colbourne (2015) conducted an experiment between ice and concrete where normal and sliding movement simultaneously act. The test was conducted with a 30-degree conical ice sample and two different concrete mixes (high and low performance) with the dimension of 1495x195x207 mm. The compressive strength of these two concrete mixes was measured at 70 MPa and 40 MPa. The sliding velocity and normal force were 180mm/s

and 10 kN, respectively. A thermal camera was used, and surface roughness was measured up to 160µm (Figure 2.8)

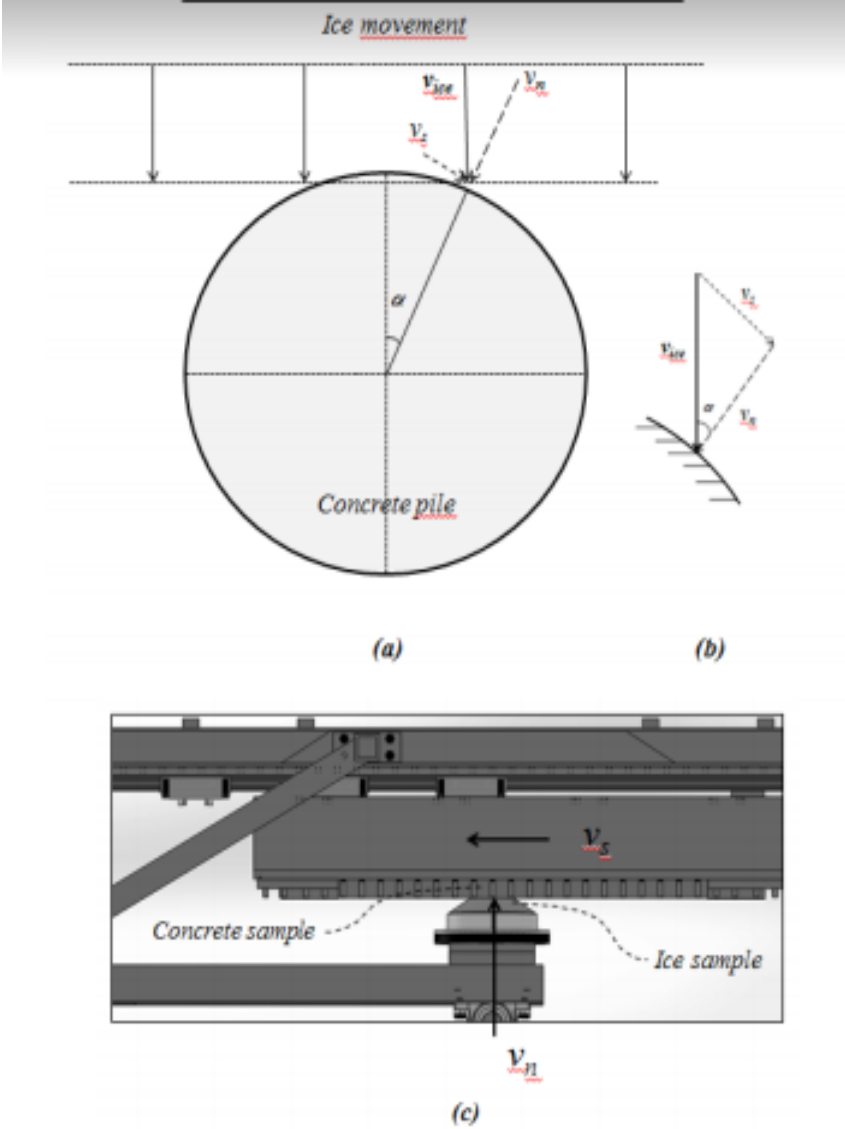


Figure 2.8: Experimental Setup (Tijssen et al., 2015)

This study showed that the abrading ice loading is a function of contact angle and ice velocity; static bonding increases with decreasing concrete surface roughness depending on the concrete mix design. Micro-scale examination showed that local thermal stress can be increased by frictional heat generation and this decreases the abrasion resistance.

2.2 Adfreeze and Pile Loading Studies

Colder region structures are oftentimes submerged in water and surrounded by sea ice covers that develop an adfreeze bond to the structure. When the water level changes, a vertical force acts on the structure, an increase in water level creates an upward force and a downward force is created with a decreasing water level. Although the impact is minimized when the water level changes are small due to the viscoelastic property of ice, this vertical force more often creates a high impact - either the ice cover is fractured, or the adfreeze bond fails as the force exceeds the adfreeze bond strength (Nakazawa et al., 1988).

Earlier Saeki (1984) Christensen (1987), Nevel (1980), Nakazawa (1988), all documented methods to calculate vertical forces acting on an offshore structure. Nakazawa used an equation, developed by Kerr (Equation 2.1) to calculate the vertical forces due to water level changes using plastic theory

$$P=2\pi a D \lambda^3 \Delta \frac{\{kei'(\lambda a)\}^2 + \{kaer'(\lambda a)\}^2}{k_1} \quad 2.1$$

Where,

$$k_1 = kei(\lambda a)ker'(\lambda a) - kei'(\lambda a)ker(\lambda a)$$

w_0 = specific weight of sea ice

D =flexural rigidity of ice plate, $D=Kh^3/12$, $K=\frac{E}{1-\nu^2}$

a = radius of structure

P = Vertical force exerted on structure

$$\lambda=(w_0/D)^{\frac{1}{4}}$$

E = Young's modulus of ice

ν =Poisson's ratio of ice

Δ =change in water level

In 1978 and 79, an investigation was conducted in Denmark to observe the damage on fixed piles and dolphins for ninety-three marinas. This examination was conducted in the winter when the average ice thickness was 0.35 m, the average pile diameter was 0.25 m, and the average tidal range was 0.2 m. The result showed, 13% of piles are displaced in a vertical direction due to the vertical sea ice force (Terahima et al., 2006) ; Baddeley (2020).

Vertical forces were found to be a serious threat for offshore structures. Although theoretical studies provided a method to calculate the vertical sea ice force, there were only a few experimental studies. Nakazawa (1988) conducted an experimental study to observe the effect of vertical ice load and adfreeze bond strength between sea ice and various construction materials, such as coated and uncoated steel piles, and old and new concrete piles with diameters of 3, 5, 10, 15, 27 and 41cm. The different pile diameters were included to evaluate the effect of structure diameter; also this study measured the effect of push out velocity, surface roughness, stress rate, ice thickness and temperature.

The experiment was conducted using push-out, pull-out and twist methods. Ice specimens were produced by cutting rectangular holes from an ice cover with dimensions of 3.2m x 1.0 m, and grain size of 8-12mm. The pile specimen was placed into the ice sample, and then turned upside-down and clamped with a steel clamp (Figure 2.9). The ice temperature was maintained the same as the air temperature and a hydraulic jack was used to control the loading rate. The adfreeze bond strength was measured by a standard load cell, and a displacement transducer was attached to the load cell to measure the pushout velocity during the experiment.

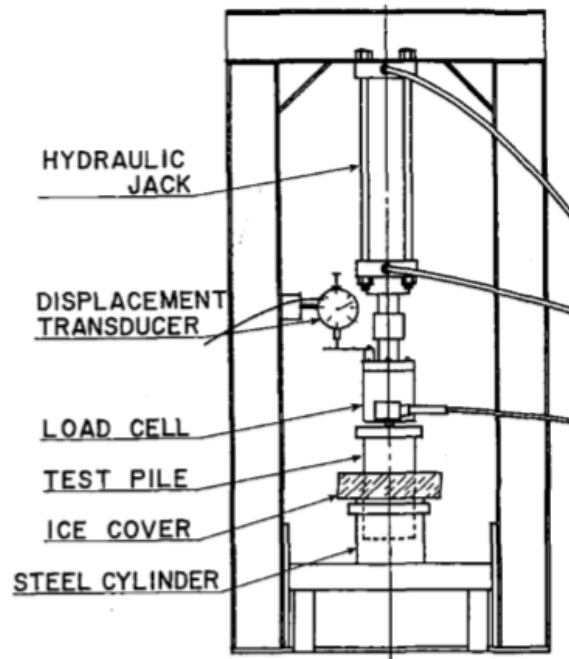


Figure 2.9: Experimental setup of Pull out test (Nakazawa et al., 1988)

The tests showed that the adfreeze bond strength depends on the construction material surface roughness and the sea ice temperature. The adfreeze bond strength increases when the ice temperature goes down. The bond strength increases when the surface roughness increases; shear strength of adfreeze bond varies between materials, and the shear force becomes higher than the adhesion force for rough surfaces. For a better understanding, it was suggested to analyze the surface roughness of construction materials. Compared to surface roughness, the effects of push-out velocity, stress rate, ice thickness, and pile diameter were found to be nominal. The bond strength increases up to a certain thickness of ice (6 cm) and then remains constant. If the pile diameter increases, the bond strength decreases.

Terahima et al. (2006) conducted field experiments where a model pile was floated in a port before the water surface froze around the test area (Figure 2.10). The experiment was conducted when the port was frozen with ice. A crane was used to provide an upward force to pull the pile through the ice and a load cell was attached between pile and crane to measure the force. The lifting force was slowly applied until the adfreeze bond failed between the pile

and the ice sheet. The ice displacement prior to failure was measured and visual findings such as cracking pattern, and the sound of failure were recorded by video.

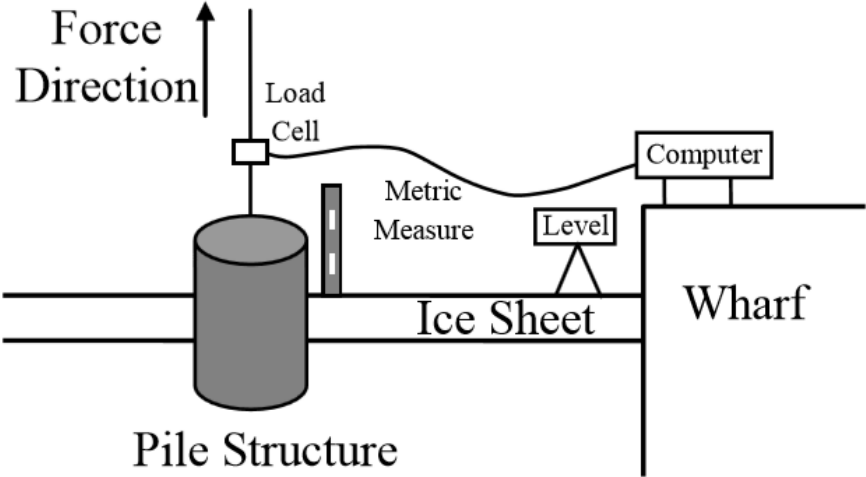


Figure 2.10: Experimental Setup (Terahima et al., 2006)

When the pull up force was applied during the test, at first six radial cracks developed through the boundary between pile and ice sheet and after that the adfreeze bond failed (Figure 2.11).

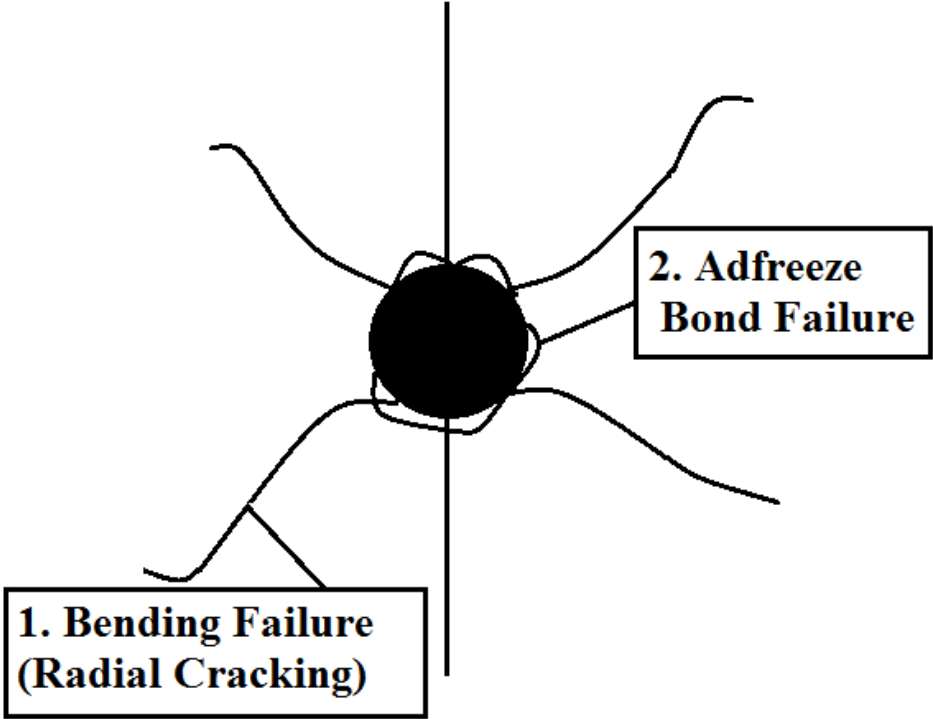


Figure 2.11: Cracks Formation During Pull-Up Test (Terahima et al., 2006)

Saeki (2011) documented experimental work to measure the vertical ice force and its effect on hydraulic and marine structures. Push-out, pullout, shear, and twist tests were performed between sea ice and uncoated rust-free steel piles with diameters of 3, 10, 15, 27, and 41 cm to measure the adfreeze bond strength and ice abrasion. An ice sheet was grown surrounding a series of test piles, and the ice sheet was then cut into samples and taken away from the field where the sample was turned upside down (Figure 2.12).

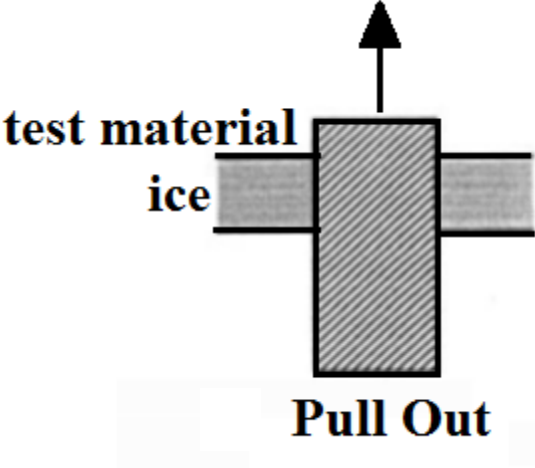


Figure 2.12: Mechanism of Pull out Experiment (Saeki, 2011)

A steel cap was inserted over the upper end of the test pile. A hydraulic jack was used to control the pullout velocity and stress rate, a displacement transducer was attached to the load cell to measure the push-out velocity, and the ice temperature was fixed at -1.7°C (Figure 2.13).

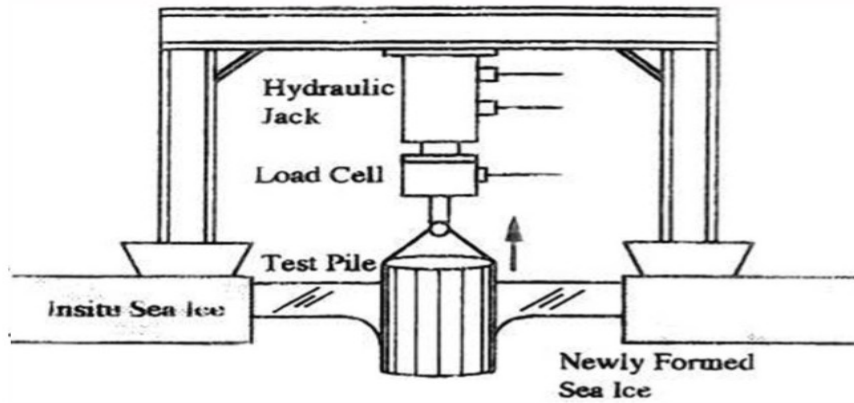


Figure 2.13: Experimental Setup to Test Adfreeze Bond (Saeiki, 2011)

The test results showed that the test procedure has a nominal impact on the adfreeze bond strength whereas the bond strength mainly depends on the pile diameter, temperature, and surface roughness. The adfreeze bond strength increases when the pile diameter or temperature decreases. When the pile diameter size is greater than 20-25 cm, the bond strength remains constant. The physical property of ice varies with temperature and the temperature of the surrounding environment. The effect of temperature is also dependent on the material surface roughness. The adfreeze bond strength changes if the surface roughness is higher than 20 μm – the bond strength increases when the surface roughness is larger (Figure 2.14).

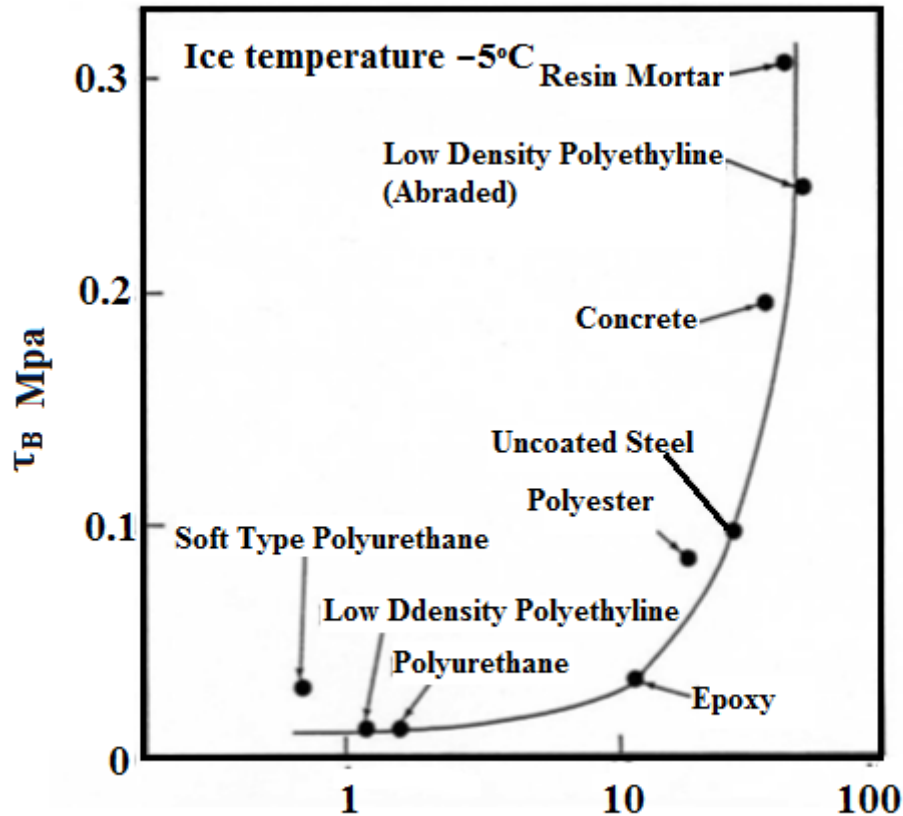


Figure 2.14: Surface Roughness Effect on Adfreeze Bond Strength of Various Materials at -5°C Temperature (Saeki 2011)

Makkonen (2012), observed that the adhesion strength is affected by temperature deviation. Especially for rigid materials, the adhesion strength was found directly proportional to the temperature; that is, the adhesion strength is stronger for higher temperatures and weaker for lower temperatures. When the temperature is near 0°C , other mechanisms override the deformation effect. As the temperature is near the melting point of ice, a liquid film of water may appear at the ice concrete interface. This film may reduce the adhesion strength. Following this theory, the ice concrete surface interaction should increase for lower temperature, unless the water film disappears.

2.3 Other Considerations of Ice Adhesion and Abrasion

Murase & Nanishi (1985) documented an experiment using freshwater ice and high-density polymer where the adfreeze bond strength was found directly proportional to the interfacial energy, that is, the bond strength increased when the energy increased. Though the experiment was conducted with a smooth surface polymer, it can be presumed that the adfreeze bond strength generally depends on the interfacial free energy. Nakazawa et al. (1988) documented work to calculate the vertical ice load where adfreeze bond strength is considered as a combination of adhesion force and the force needed to shear the ice embedded in the construction material. This study concluded that the adfreeze bond is heavily influenced by the surface roughness.

In 1988, a field study was conducted along the Swedish coast at more than 30 lighthouses to investigate the effect of floating sea ice. These lighthouses were widely spread in the coastal area and exposed to various ice and water conditions responsible for different structural damage types. There was no abrasion found where the level ice thickness was less than or equal to 0.3m, and the abrasion rate was found more critical for harsh environments, where the ice level ice thickness exceeded 0.3 m thickness. More serious damage was generally observed below the water line, and the average abrasion rate was 0-140 mm/year (Møen et al., 2008).

The chemical reaction between seawater and concrete can cause other damage. Water and chloride penetration can dissolve the lime in concrete and this increases the permeability of concrete. The sulphate in seawater may react with wet cement particles, which can weaken the concrete (Huovinen, 1990) (Figure 2.15).

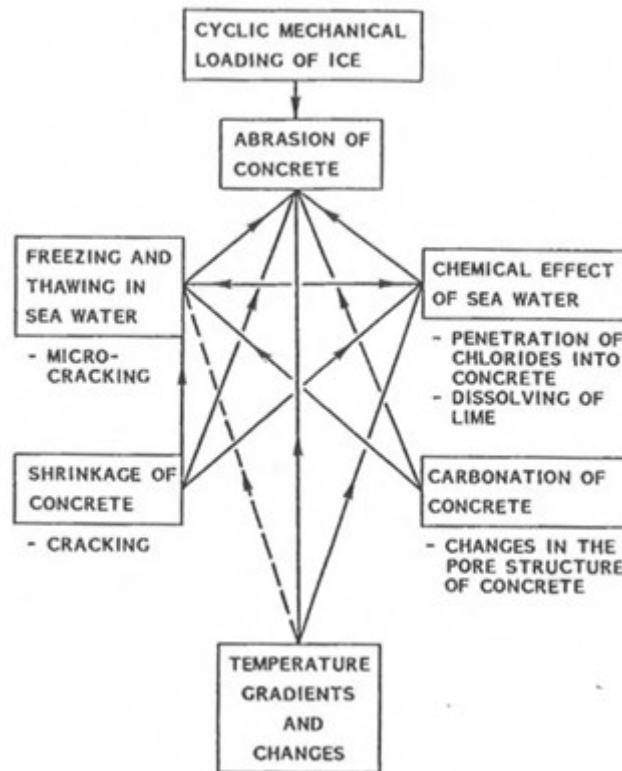


Figure 2.15: Effect Causing Damages to Concrete in Sea Ice (Huovinen, 1990)

To observe the arctic environment effect and corresponding concrete abrasion, A field experiment was conducted at a dock of Nanisivik, Baffin Island, Canada. This field study covered seven years, where 12 panels were designed with 12 different concrete mixes and exposed to the environment throughout this period (Møen et al., 2008). By visual and microstructure examination, the yearly rate of concrete abrasion was found to be nominal (0-7 mm/year), except for some local corrosion in steel fibres used for fiber-reinforced mix design. No definite reason was found for this lower abrasion rate.

Saeki (2011) conducted experiments and compared the concrete abrasion due to sea ice and freshwater ice. The experiment used concrete samples of different strength and with different aggregates under various temperatures and vertical pressures. For both types of ice samples, the wear rate had a similar linear relationship with the vertical stress. There was no difference in average concrete abrasion rate when the temperature was higher than -10°C , while if the

temperature was below -20°C , the mean abrasion rate from sea ice was found to be higher than that from the freshwater ice (Saeki, 2011).

Salt in seawater ice increases the abrasion rate, and a similar impact was observed for freshwater ice if it contains particles such as clay, sand, powdered concrete, etc. (Hiroshi Saeki, 2011). In 1991, Tachibana collected different ice samples containing particles with different diameters and distributed them in groups by their average diameter. The relative velocity of the ice movement was 5cm/s ; ice temperature was -10°C , and the median diameters of sand particles were 0.03 , 0.14 , and 0.7 mm. The result of this experiment showed that ice containing solid particles is much more aggressive for concrete abrasion than pure ice (Saeki, 2011).

For pure water, the ice to substrate interface forms at the freezing temperature (Makkonen, 2012). When the thermal coefficient of ice and the material is different, the difference in thermal contraction of the ice and the material can initiate failure of the joint at the interface. The ice and the solid material may have different cooling rates due to different heat capacity and thermal conduction, thus causing additional stress at the interface. As ice is able to creep, this stress depends upon the cooling rate.

When ice comes in contact with a submerged concrete structure, ice creates pressure in the concrete pores and is responsible for increasing the pore pressure in the concrete, which causes structural damages (Jacobsen et al., 2015).

Figure 2.16 shows a schematic diagram of concrete (column) abrasion due to sea ice (sheet) collision while moving from left to right. Three different regions are identified. High normal stresses are imposed on ice and concrete in region 1, where the water layer between them is pushing against both surfaces. The crushing and fragmentation are observed near the concrete column, and microscopic cracks are formed in the upstream direction. The maximum abrasion

is obtained in region 2, where normal forces are decreased, and shear forces increased, and debris is found near the column. Normal stress is minimal in region three, but a large amount of debris is also observed. It is assumed that the damage mechanism is different in this region compared to the previous areas.

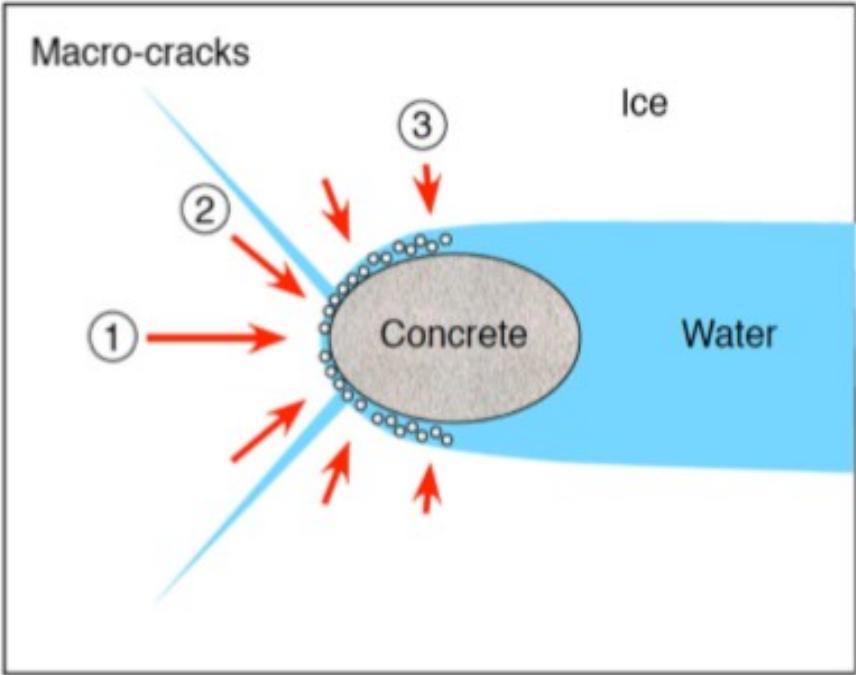


Figure 2.16: Schematic Diagram of Concrete Abrasion Mechanism (Jacobsen et al., 2015)

2.3.1 Ice Adhesion Theory

Theoretically, the ice adhesion mechanism can be explained in several ways. In 2011, Lasse Makkonen described the basic theory of ice adhesion using the mechanism of the water contact angle on a surface (Makkonen, 2012). Figure 2.17 shows a schematic diagram where a drop of water (w) is on a solid surface(s) with an interface of (w,s). Where,

The contact angle of droplet is θ

Corresponding surface energy is γ

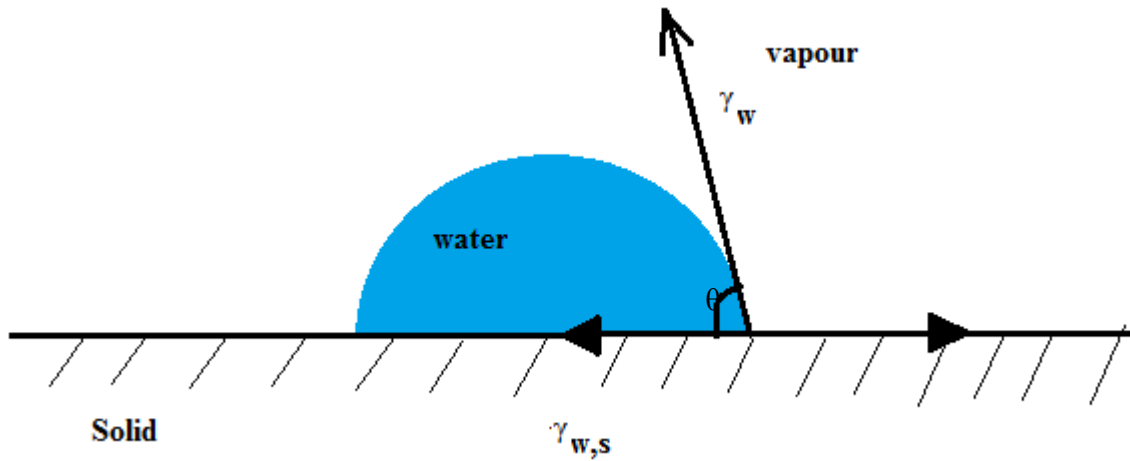


Figure 2.17: Water Drop on Solid Surface and definition of Contact angle (Makkonen, 2012)

The Young equation of equilibrium for this case is

$$\gamma_{w,s} + \gamma_w \cos\theta = \gamma_s \quad 2.2$$

If the droplet is assumed to be frozen into ice on the surface, the work needed to break the adhesion bond and form two new surfaces (ice and solid) in the absence of deformation, will be defined as the thermodynamic work of adhesion (W_a)

$$W_a = \gamma_s + \gamma_i - \gamma_{i,s} \quad 2.3$$

Inserting the value of Equation 2.2 into Equation 2.3 we get

$$W_a = \gamma_i + \gamma \cos\theta + (\gamma_{w,s} - \gamma_{i,s}) \quad 2.4$$

Now assuming the surface energies of water and ice are approximately equal, and considering the interfacial energies at the solid surface approximately equal, the equation 2.5 is obtained

$$W_a \approx \gamma_w (1 + \cos\theta) \quad 2.5$$

Equation 2.5 represents that the thermodynamic work of ice adhesion and is nearly equal to the surface tension and contact angle of the water on the solid material. This mathematical expression shows that ideally, ice adhesion is mostly dependent on the work of adhesion and

contact angle of water. However, macro scale experiments have shown that the material deformation or the ice-solid contact is complex and dependent on various other factors such as salinity, crystal structure of the ice, and surface roughness of the material.

The work (W_s) spent to separate an interface of two surfaces using a perpendicular force $F(x)$, is described as

$$W_s = \int_0^{\delta_x} F(x) dx \quad 2.6$$

Where, δx is the distance at which the surfaces are considered to be ‘separated’. Here both W_s and $F(x)$ are defined per unit area of the original interface if the surfaces are perfectly smooth. As the atomic forces decrease very rapidly with distance, the δ_x will be at molecular scale.

For the ideal case, when the surface of the material is perfectly smooth, and the material is rigid, the mechanical work spent will equal the thermodynamic work of adhesion. However, in reality, the mechanical work required to pull the ice away from the surface is typically much higher than the thermodynamic work. Intermolecular interactions may be responsible for this phenomenon.

The material surfaces are deformed due to adhesion failure. This deformation can be brittle or ductile, and ice itself also fails in both modes. The elastic modulus of ice strongly depends on the temperature; the true ice removal distance can also be higher than the theoretical. The failure mechanism of ice may also change with the flexibility of the surface interface. If the surface material is highly elastic and/or the temperature is near the melting point, the ice interface behaves like a ductile material. While brittle behaviour was observed with the rigid surface and/or cold ice sample (Makkonen, 2012). Theoretically, the temperature affects the perpendicular force used to separate the ice from a solid surface.

Jacobsen explained the ice-concrete adhesion bond for vertical structures using Hertzian theory (Jacobsen et al., 2015). Figure 2.18 shows a schematic diagram of an ice-concrete interface where the ice sheet moves towards the concrete surface with water in between. The ice concrete interface was simplified by drawing half spheres that represents the irregular surface of ice hitting the concrete structure, where ‘a’ is the radius and F is the reaction force from each half-sphere.

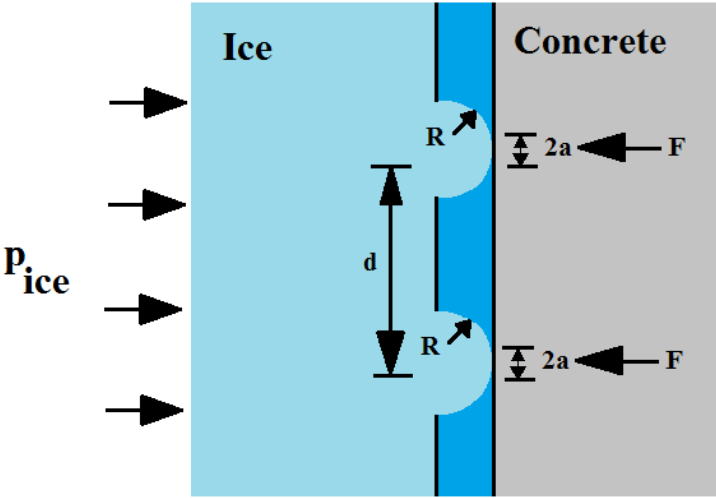


Figure 2.18: Simplified Illustration of Ice-Concrete Interface for a Vertical Concrete Structure (Jacobsen et al., 2015)

The mean ice pressure and the mean contact pressure were considered as p_{ice} and p_0 . According to the ideal Hertzian theory, the mean contact pressure is 2/3 of the maximum contact pressure p_0 , that is-

$$p_m = \frac{2}{3} p_0 = \frac{F}{\pi a^2} \tag{2.7}$$

- Where p_m = mean contact pressure
- p_0 = maximum contact pressure
- F = reaction force
- a = radius of contact area.

It is assumed that there is no water between the surfaces and the ice edges are directly adhering to a flat concrete surface using the Hertzian contact pressure. The radius of the contact surface is derived as

$$a^3 = \frac{3FR}{4E^*} \quad 2.8$$

Where R= radius of asperity
E* = reduced modulus of elasticity

$$\frac{1}{E^*} = \frac{1-\nu_i^2}{E_i} + \frac{1-\nu_c^2}{E_c} \quad 2.9$$

Where,
 ν_i^2 = Poisson's ratio of ice
 ν_c^2 = Poisson's ratio of concrete
 E_i = Young's modulus of ice
 E_c = Young's modulus of concrete

Using the following equations, the ice concrete contact radius for the particular surface roughness radius can be determined from the applied force of ice on the contact area. When the environmental temperature is cold enough to avoid melting, the mean contact pressure over the contact area πa^2 is limited by the compressive strength of ice, that is

$$F \leq \pi a^2 f_{c,ice} \quad 2.10$$

Using equation 2.8

$$A \leq \frac{3\pi R f_{c,ice}}{4E^*} \quad 2.11$$

where $f_{c,ice}$ = compressive strength of ice

Equation 2.11 shows that the contact radius non-linearly increases with ice strength where the E* varies with different ice concrete combinations and contact radius is considered just before the ice crushed. Once the ice is crushed, the contact point no longer exists and the ice rubble is forced into surface pores or extruded along the concrete surface.

Makkonen (2012) found that minute bubbles of air in the ice-material interface can reduce the true interface area, and the adhesion bond strength decreases. On the other hand, the actual interface area is larger than the apparent area when the surface is rough on a microscopic scale, and the micro-pores of the surface are filled with water also, water droplets easily penetrate into the micro-pores of the material surface and freeze into the pore structure of the material.

2.4 Summary of the State of the Art Regarding Ice Bonding and Concrete Wear

In colder regions, one of the primary reasons behind marine structural concrete surface abrasion is ice interaction. Abrasions are found near or at the waterline for concrete structures such as lighthouses, docks, bridge piers, or guide walls. The effective magnitude of the local ice force depends mostly on the strain rate, salinity, crystal orientation, and temperature. Marine structures can experience severe damage sometimes removing all the concrete cover at the waterline due to moving ice (B. C. Gerwick, 1988).

In order to observe the concrete abrasion mechanism and the wear rate accurately, the ice load and concrete resistance need to be measured. Both ice and concrete physical and mechanical properties need to be measured as part of either field or laboratory studies. In addition the physical characteristics of the interaction need to be carefully considered before a test plan is developed and recorded during experimentation (Barker et al., 2019) (Jacobsen et al., 2015).

In general, there has been substantial investigation of ice adhesion, ice friction and concrete wear arising from dynamic interactions with ice. There has however been relatively little study of static bonding of ice to concrete leading to material loss at separation.

2.5 Rationale for this Study

Based on the review of previous investigations it is found that the wear associated with adhesion has not been extensively studied. This study provides an experimental investigation

of concrete adhesion and abrasion due to normal surface bonding and subsequent tensile separation between ice and concrete. The laboratory set up was developed and the experimental parameters for both ice and concrete samples were planned so as to measure bond strength and abrasion more accurately. The details of the experimental program are described in chapters 3 and 4.

Chapter 3 : Experiment Criteria, Design and Implementation

This chapter presents the design concept for the experiment to measure the adfreeze bond strength at an ice concrete interface at laboratory scale. The design criteria and rationale are explained in detail. The implementation and operation of the apparatus are described in the next chapter

3.1 Design Criteria of Apparatus

A standardized experimental study is established to measure ice concrete adhesion and the corresponding material removal mechanisms. Based on the review of previous studies and following the objective of investigating adhesion based wear, this study developed a simple experiment to measure the adhesion of ice to concrete with standardized specimens (both ice and concrete samples) under a controlled environment. The apparatus can conduct the trials efficiently and accurately under a range of realistic pressures and time durations.

Based on the literature survey (Chapter 2) the following features and factors are incorporated into the apparatus: constant long term applied pressure, continuous measurement of applied normal force and bond breaking force, the ability to perform dry and submerged tests, use of different ice type samples, use of different concrete, stone or cement samples, control of the bond breaking rate, temperature control, and measurement of material loss from the concrete samples. These criteria or capabilities are discussed further in the following sections.

3.1.1 Velocity –Loading Rate, Start- Stop, Adhesion

Previous studies have shown ice concrete bonding under vertical loading, and depending on the duration, significant reverse directional force is required to separate the ice and concrete samples (Saeki, 2011). Nakazawa conducted a push-out test between ice and steel piles under varying loads and rates; nominal changes were found in the adfreeze bond while the push-out velocity ranged from 0.001 to 10 mm/s. However, previous studies determined that the

adhesion bond slightly decreases with the decreasing push-out velocity (Nakazawa et al., 1988) .

This study is designed to provide an uncomplicated measurement of tensile bonding. Towards this goal, most variables are controlled to be as simple as possible. The applied load is a constant during each individual experiment. The second variable is the contact duration. The concrete specimen is pulled away from the ice using a single constant withdrawal rate of approximately 4mm/sec. The applied pressure and bond strength are both measured using the same 1000 lb load cell. The separation loading rate is controlled using a hand-held power drill driving a scissor jack. Each of these variables and other parameters that were considered as part of the experimental planning are discussed in the sections following.

3.1.2 Applied Pressure

Adfreeze bond strength is one of the significant parameters for vertical ice load measurement. Shear or tension forces can both be evident in the adfreeze bond interface between ice and another material (Figure 3.1).

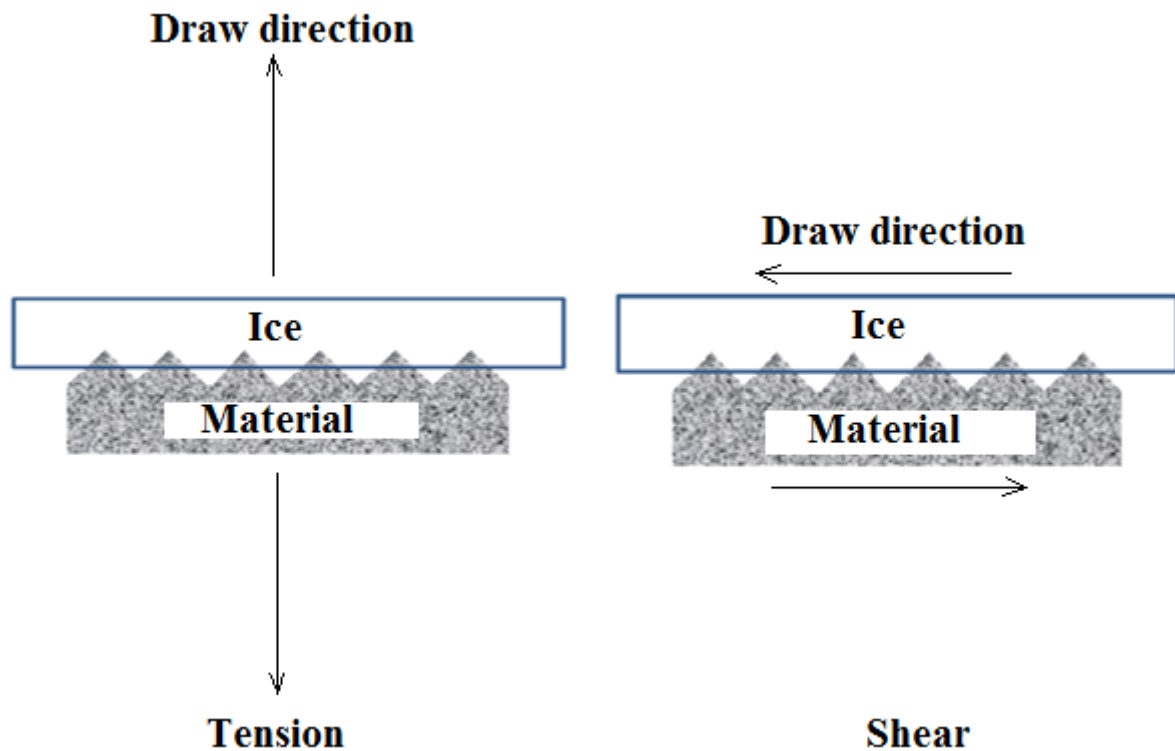


Figure 3.1: Mechanism of Ice adhesion to a Material surface (Saeki, 2011)

If the force is acting vertically, that is tension; the interfacial free energy controls the adfreeze bond strength between the material surface and ice. This bond strength deviates with the rough surface of the material and the actual contact area of ice (Saeki, 2011).

Previous studies indicate that the adfreeze bond strength significantly depends on the contact area or the adfrozen area (Saeki, 2011) whereas the abrasion rate increases with increasing contact pressure (Y. Itoh et al., 1988). The adfreeze bond strength decreases with increasing diameter of contact material up to 20-25 cm diameter; after that, it remains constant. The maximum contact pressure was observed to be 2 MPa for the concrete sample diameter ranges from 3-41 cm (Saeki, 2011). The equipment used in this experiment was initially designed to exceed this maximum (2MPa) pressure on a concrete sample 30 mm in diameter. However on the concrete sample size was later changed to standardized samples that are 50.8 mm in diameter which results in an upper pressure limit of around 1MPa..

3.1.3 Dry and Submerged Tests

Previous experimental work has focussed largely on dry tests with vertical loading between ice and the other material. However it has been observed that, much of the ice induced wear on concrete structures occurs just below the waterline (Møen et al., 2008). Thus the water at the ice concrete interface is a factor when looking at adhesion bonding. The presence of fluid may affect the concrete wear rate, induce cracks and be responsible for reducing the life of the concrete (Huovinen, 1990). Although Jacobsen (Jacobsen et al., 2015) has theoretically explained the fluid effect at the ice concrete interface, an experimental investigation has not yet been presented. To investigate the abrasion mechanism thoroughly the apparatus was designed to allow both dry and submerged tests.

3.1.4 Ice Type

Most previous studies have been conducted with freshwater ice rather than saline ice, as brine pockets in saline ice increase the surface roughness and probably increase the wear rate (Y. Itoh et al., 1988). One earlier experiment was conducted with freshwater ice samples collected from the field (Lake Soroma) (H. Saeki et al., 1984). One reason for using these natural lake-ice samples was the unidirectional crystal structure, which is similar to sea ice but without the brine. This helps simplify the experiment. Later experiments were designed with laboratory made fresh water ice samples (Fiorio, 2005), (Fiorio et al., 2002), (Jacobsen et al., 2015) and (Møen et al., 2015).

The reason for using laboratory-made fresh water ice is the opportunity to reproduce more consistent and standardized ice samples for repeated tests. An initial investigation of adfreeze bond strength would be more difficult with ice samples having varying degrees of salinity or other characteristics. The current study was designed with laboratory made standardized polycrystalline freshwater ice samples (described detail in chapter 4). The pH of the ice was

also measured and grain structure analysis was conducted for a subset of the ice samples to test for consistency.

3.1.5 Concrete Type

Ice adhesion is significantly dependent on surface roughness and material properties (Saeki et al., 1985). Depending on the modulus of elasticity and Poisson ratio of the ice and concrete samples, the adfreeze bond strength can vary significantly. Therefore it is likely that wear rate can also fluctuate (Jacobsen et al., 2015). The aggregate type or presence of steel fiber, and the cement mix design, all influence the abrasion mechanism (Y. Itoh et al., 1988),(Greaker, 2014). Similar to the desire for a consistent ice sample, a single mid-strength concrete mix was used. In general, the mid-strength concrete is used in marine structures, marinas and harbor areas. The abrasion characteristics of this particular mix is expected to be used as a reference for comparison with other concrete mixes in future.

3.1.6 Temperature

Ice adhesion is dependent on the ambient or interface temperature, and thus temperature needs to be controlled during an experiment. Several previous experimental studies were conducted inside cold rooms at temperatures ranging from -5 to -20 °C (Yoshishige Itoh et al., 1994), (Fiorio et al., 2002), (Fiorio, 2005), (Hiroshi Saeki, 2011), (Tijssen et al., 2015), (Møen et al., 2015), (Bekker et al., 2011), (Amanda Ryan & John, 2018). It is essential to maintain a constant subzero temperature to prevent the ice melting. Earlier, Sodhi (D. S. Sodhi, 2001) demonstrated that floating pack ice near the water line exists at a temperature close to the melting point. Thus the ideal temperature for experimenting is near 0 C for dry and wet conditions. The dry test is designed for a controlled temperature of -1°C. For the submerged test, it is challenging to stop the water from freezing when the temperature is subzero. The submerged experiment is designed to be conducted at 0C. Both types of experiment are conducted inside a cold room with constant temperature during the experiment. The sample

and apparatus are placed inside the cooldroom 24 hours before the experiment to avoid temperature variation.

3.1.7 Measurement of Applied Pressure and Adfreeze Bond Strength

Measuring the contact pressure and adfreeze bond strength is an essential part of this study. Previously, most studies used a standard load cell for measurement (Y. Itoh et al., 1988), (Nakazawa et al., 1988), (Saeki, 2011). This study uses a 1000 lb (4500N) load cell incorporated into the apparatus. The measuring equipment is placed inside the cold room with data recorded from outside the cold room using National Instruments Data Acquisition System and NI Labnet software.

3.1.8 Measurement of Concrete Abrasion

Various methods have been applied previously to obtain the concrete abrasion extent. The ice to concrete contact area changes significantly once the ice is crushed against the concrete surface (Jacobsen et al., 2015), (Amanda Ryan & John, 2018). During the interaction, concrete particles are also crushed against the ice debris and embedded in the ice surface. For the dry test: the abrasion can be measured either by melting the ice and collecting the embedded concrete or by taking photographs, depending on the amount of wear and dimension of the ice sample. In the case of a submerged testing, it is more difficult to collect the abraded concrete particles as there is a good chance that the concrete particles may be dispersed in the water. Alternately the surface roughness of the concrete samples can be measured before and after the experiment to observe the change in surface profile due to ice adhesion. At large scale, the standard way to measure the abrasion is by measuring the concrete weight before and after the experiment. This study has done a combination of each of these methods as a means of comparing the different methods and possibly determining which of the methods provides best results.

3.1.9 Examination of Coarse Aggregate Rock Core and Cement Paste

Prior studies have explained that the adhesion of ice depends on the surface roughness and varies with the concrete mix design. It was observed that the adfreeze bond strength varies across the surface of a sample with different levels of adhesion with exposed concrete aggregate and the areas of concrete paste. The mix design used for this study has a combination of coarse aggregate from three different rock types. To analyse the adhesion with each of the concrete components, in detail, it was decided to conduct additional adhesion experiments under varying pressure and temperature with samples of the three different rock types and a sample made with only cement paste.

3.1.10 Loading and Unloading

The experiment was designed to load the concrete sample against the ice under constant pressure for a long period of time and then pull it off by applying a reverse direction force after the time duration. Previous pile studies have used a hydraulic jack to apply the negative loading for vertically pulling out the samples from the ice specimen (Hiroshi Saeki, 2011). In the current study the contact pressure is applied using weight bars. A scissor jack is used to apply the separation force, lifting both the weight bars and the bonded sample. A hook was designed with one end attached to a standard hand power drill and other end attached to the jack. The drill speed controlled the separation loading rate through the scissor jack.

3.1.11 Summary of Design Criteria

Table 3.1 provides a summary of the design requirement and criteria. The application of these criteria in developing the apparatus and experimental plan are described in detail following.

Table 3.1: Design Requirement and Criteria

Determined Design Requirement	Design Criteria
1. Load and rate	Constant load application during bonding phase and a controlled reverse load rate for bond breaking
2. Pressure	Maximum applied pressure of 1 MPa
3. Dry and Submerged Test	Dry and submerged test set up accommodation in the design
4. Ice Type	Laboratory made freshwater ice that can repeatedly reproduced with consistent properties
5. Concrete Type	Mid-Strength standardized mix design
6. Temperature	Controlled temperature for dry and submerged test
7. Measurement of Applied Pressure and Adfreeze Bond Strength	1000lb load cell was used to record and collect the pressure during the experiment
8. Measurement of Concrete abrasion	Recording the concrete sample weight before and after the experiment, taking photograph and collecting abraded particles from the ice surface if possible
9. Examination of Coarse aggregate Rock Core and Cement Paste	Conducting experiments with rock cores and cement paste samples to examine differences in adhesion for components of the concrete matrix

3.2 Concept Design

Based on the design guidelines, several introductory concepts were evaluated in the course of developing the device features. Most prior studies have used relatively large scale laboratory experiments. Based on the available laboratory space, cold room dimensions and a desire to

keep the sample size manageable, this study elected to conduct small scale experiments. An off-the-shelf apparatus was initially selected for pilot experiments. This apparatus meets the ASTM D7234 - 19 standard test method for pull-off adhesion strength of coatings on concrete using portable pull-off adhesion testers.

However this apparatus presented practical difficulties as it required a separate load application mechanism and a somewhat difficult attachment of the pull-off actuator. These initial observations lead to a custom apparatus design to reduce the problems observed with the off-the-shelf equipment.

The ice sample was chosen to be clamped to the base of the apparatus and to remain fixed during the experiment as ice is sensitive to the temperature and easily deformed under pressure. Both ice and concrete samples were cast in cylindrical shapes, with the ice sample much larger than the concrete sample. In both cases the cylinder shapes allowed the samples to be easily clamped without unduly stressing the samples.

Also it is relatively easy to analyze the face surface of a cylinder compared to other geometric shapes.

The concrete diameter was chosen to be 50.8mm while the ice diameter was 226mm. The smaller concrete diameter allowed investigation of the effect of the adfreeze bond, indentation, and creep on the larger ice surface beyond the exact contact area.

Also this is the smallest standard specimen size for concrete according to ASTM 192. The smallest size furnishes the highest contact pressures for a given load and the load size determines the size and strength of the apparatus.

It was necessary to clamp the concrete sample, attaching the load cell without affecting the concrete surface. An aluminium clamp was designed to hold 2/3 of the length of the sample

and keep the rest of the sample exposed for observing the interaction with the ice. The cylindrical holder also distributed the downward load evenly around the circumference of the sample so that load eccentricities were avoided and uniform contact pressures were assured. Before the test, the concrete cylinder in its holder was attached to the load cell. The concrete cylinder was then put in contact with the ice surface and pressure applied for the specified time period. The samples were finally pulled apart by reverse loading after the stated time (Figure 3.2). The applied pressure and the bond strength (adhesion pressure) were both measured by the attached load cell without a need to change attachments or affecting the concrete sample.

The concrete sample temperature was the same as the ice sample for both dry and submerged tests. The concrete specimen was dry during the dry test; for the submerged test, the water temperature remained at 0.1° C to prevent freezing.

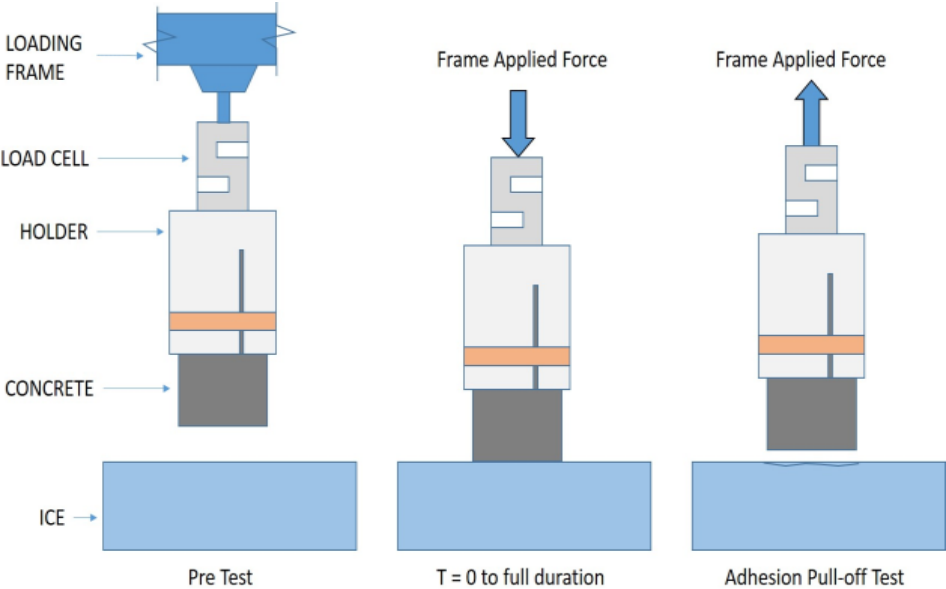


Figure 3.2: Basic Mechanism of Experimental Setup

As past studies have observed that impurities in water can affect the adfreeze bond strength, distilled and deionized water was used for submerged tests to prevent this influence.

The aggregate only sample and the paste only sample were shaped to the same dimensions of the concrete cylinders and tested in the same way as the concrete samples.

Chapter 4 : Experiment and Analysis

This chapter describes the methodology of the pilot experiment, the subsequent main experiment, data collection procedure, data analysis, and significant findings.

At first, a pilot experiment was conducted. Based on the results of the pilot experiment, the main experiment was improved and refined with more useable equipment and a simpler instrumentation setup. The main experiment was designed for both dry and submerged tests and to allow testing the rock samples of the aggregate used in the concrete mix design. The collected data were statistically analyzed and plotted. The significant findings are noted in this chapter, whereas discussion and recommendation are described in the next chapter.

4.1 Pilot Experiment

Prior to finally designing the equipment for the laboratory experiment, a pilot experiment was designed to explore various aspects of the experiment and the procedures including the size and shapes of the standardized ice and concrete specimens. These pilot experiments were conducted to get some ideas about the expected levels of adfreeze bond strength, and to explore procedures for preparing specimens, attaching instrumentation, applying loads and in particular the issue of effecting a long term positive load followed by a very short term negative load through the same samples. The main experimental setup was designed according to these pilot findings in terms of improving the efficiency of the experimental process, maximizing the quality of measured results and minimizing the potential for errors.

The pilot experiment process was conducted as follows. A freshwater ice sample was produced, cut to size, and placed on a table. A concrete cylinder was smoothed on one face, inserted in an aluminum clamp holder, and placed over the ice sample for a certain duration of time. Weight bars were placed on top of the concrete sample for a constant compressive load (Figure 4.1). After a specified duration, the weight bars were manually removed, a threaded

rod was attached to the aluminum clamp, and the concrete sample was pulled away from the ice using a Posi Test Machine that is more commonly used for testing paint adhesion. This pilot experiment provided load measurements and some procedural experience that were used as guidelines for designing the main experiment.

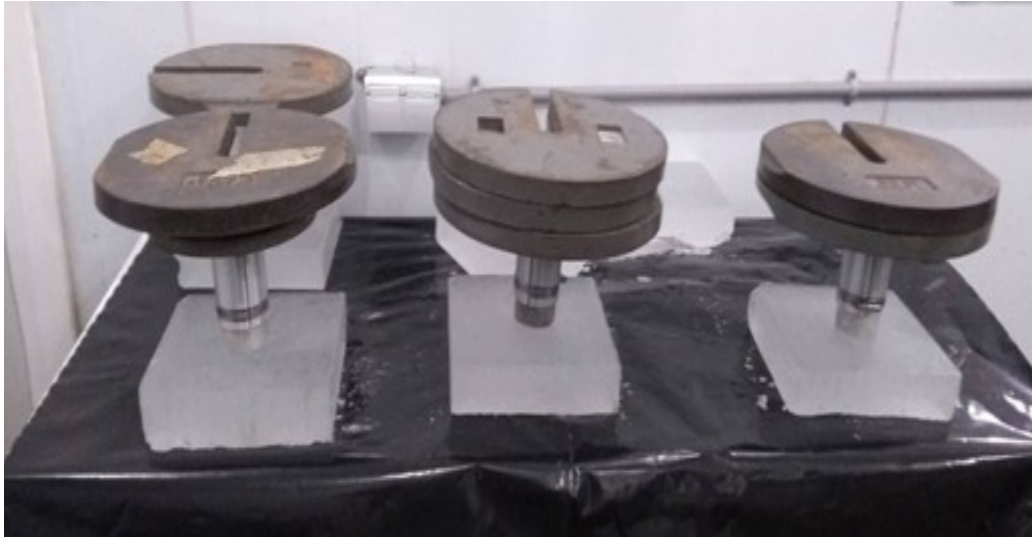


Figure 4.1: Pilot Experimental Setup

The key reason of selecting the experimental temperature (-1°C) was to conduct the experiment closer to the temperature of real life cases. To compare the adhesion bond strength under various temperatures, the pilot test was conducted at three different temperatures -1°C , -10°C , -15°C . It was observed that the bond strength is directly proportional to the temperature. That is the bond strength for a given duration of contact is weaker for lower temperatures. As the scale of the current experiment is relatively small, almost no adhesion bond was observed for -10 and -15°C . So the temperature was further confirmed to be more appropriate at -1°C .

Pack ice is more likely to move with tides or with changes in wind, and river ice commonly moves with the current during periods of most active abrasion. The experiment was designed for time durations of applied pressure in the range between 5-120 minutes based on an estimation that this was a reasonable range of time periods for these natural phenomena.

For short duration bonding experiments, the adfreeze bond strength was found to be very weak and easily broken by the handling required to attach the Posi-Test Machine. Hence the need to have minimal handling between the changeover from positive loading to negative loading during the experiment was identified as a key factor for the success of the experiment.

4.2 Surface Interaction

An indentation was regularly observed in the ice sample after an extended duration test, and even after a short test with higher contact pressure. The indentation has almost the same radius as the concrete sample (Figure 4.2). In cases where the bond strength is higher, minor cracks or material loss were observed around the circumference of the indentation. Thus the ice sample dimension was chosen to be larger than the concrete specimen, so the additional cracking or material loss in the contact area and peripheral area of the ice sample can be observed after the experiment.

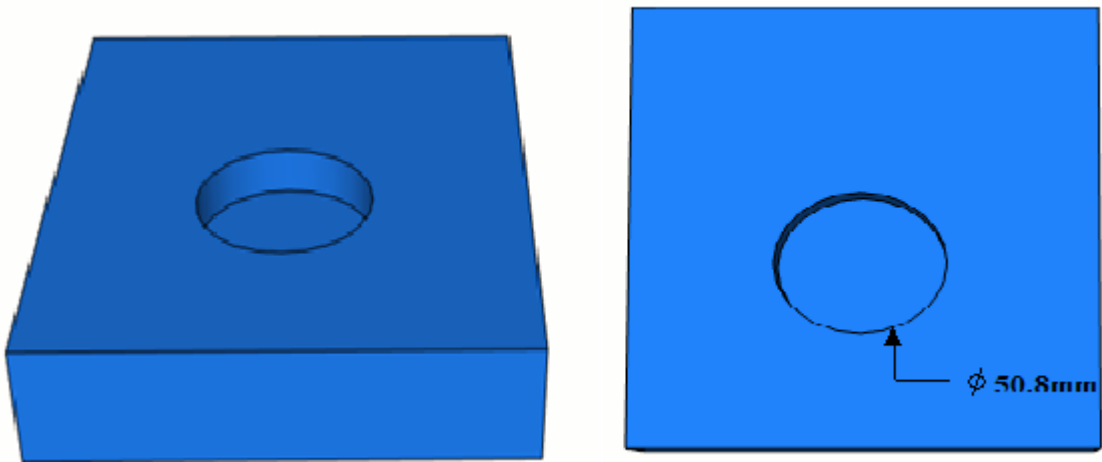


Figure 4.2: Surface Indentation

4.3 Sample Preparation

4.3.1 Ice Samples

Individual ice features, such as origin, strength, and thickness, have a significant impact on concrete abrasion (Shamsutdinova, Hendriks and Jacobsen, 2015) and water salinity and impurities impact the strength of ice. This study used standardized freshwater ice samples to fit with existing concrete sample production and testing equipment.

The key reasons for using freshwater ice are:

- Fresh water ice eliminates the variables that would be introduced by the presence of salt, thus using the freshwater ice sample reduces the dimensions of the experimental matrix and avoids a source of variability.
- Reproducing saline ice in the laboratory is a complicated process, and it is hard to replicate the same microcrystal properties for each of the samples, whereas, for freshwater ice, it is comparatively simple to reproduce the same ice samples for multiple times.

The ice samples were produced in the laboratory following a method, documented in earlier work (Bruneau et al., 2013). This preparation method is a standardized procedure for producing ice samples with consistent mechanical properties and internal structures that can be reasonably considered as a replica of natural freshwater ice that is polycrystalline and anisotropic. The ice was prepared with seeded ice and water using a unidirectional freezing method (Figure 4.3.) that minimizes the generation of internal stresses and trapped air that would be caused if the ice was allowed to freeze from multiple directions.

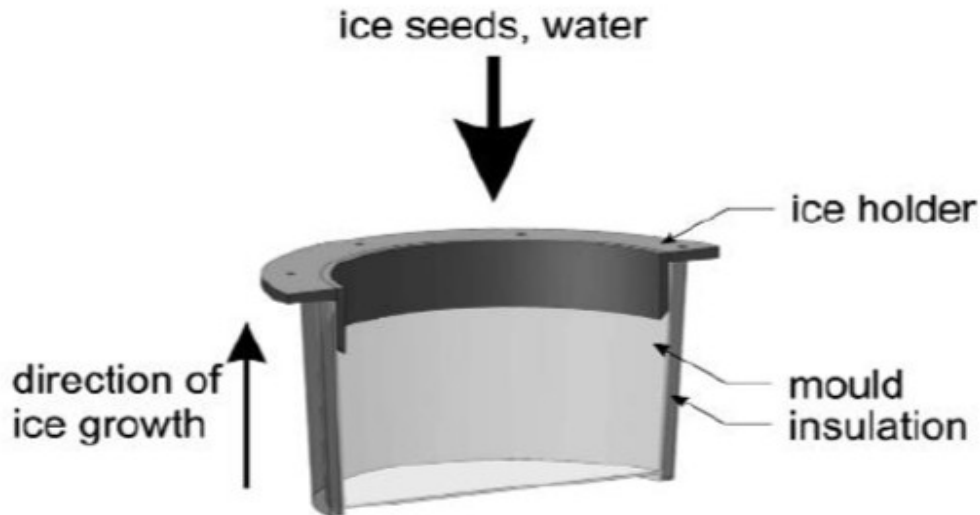


Figure 4.3: Schematic Diagram of Ice Preparation (Bruneau et al., 2013)

Commercial ice cubes were crushed mechanically to obtain the ice seeds, which are then mixed with deaerated, deionized, distilled water by stirring them together to mix them uniformly. The ice-water mixture was prepared in a cylindrical container and support frame designed to fit in the test apparatus. The sides of the ice container were insulated and the bottom extended into a deep freezer at -15 to -20 °C to allow for freezing the ice sample unidirectionally from the bottom up. This method avoids cracks and flaws associated with air and liquid water being trapped inside the freezing front. Once the samples were completely frozen, they were demoulded by slowly pouring room temperature water over the outer surface of the steel container, until the ice sample released (Figure 4.4).

After demoulding, the ice samples were turned upside down and rubbed over an aluminum plate to smooth and flatten the ice surface. The sample surface was wiped with a clean cloth to remove any excess water on the top layer, wrapped in a plastic bag to protect the sample from moisture and evaporation during storage and kept inside the cold room. The ice sample dimensions were constant at 228.6 mm diameter and 101.6 mm height (Figure 4.5). The ice sample size was selected on the basis of having a surface that was continuous at least one full

sample diameter beyond the contact point so as to eliminate the possibility of edge or boundary effects

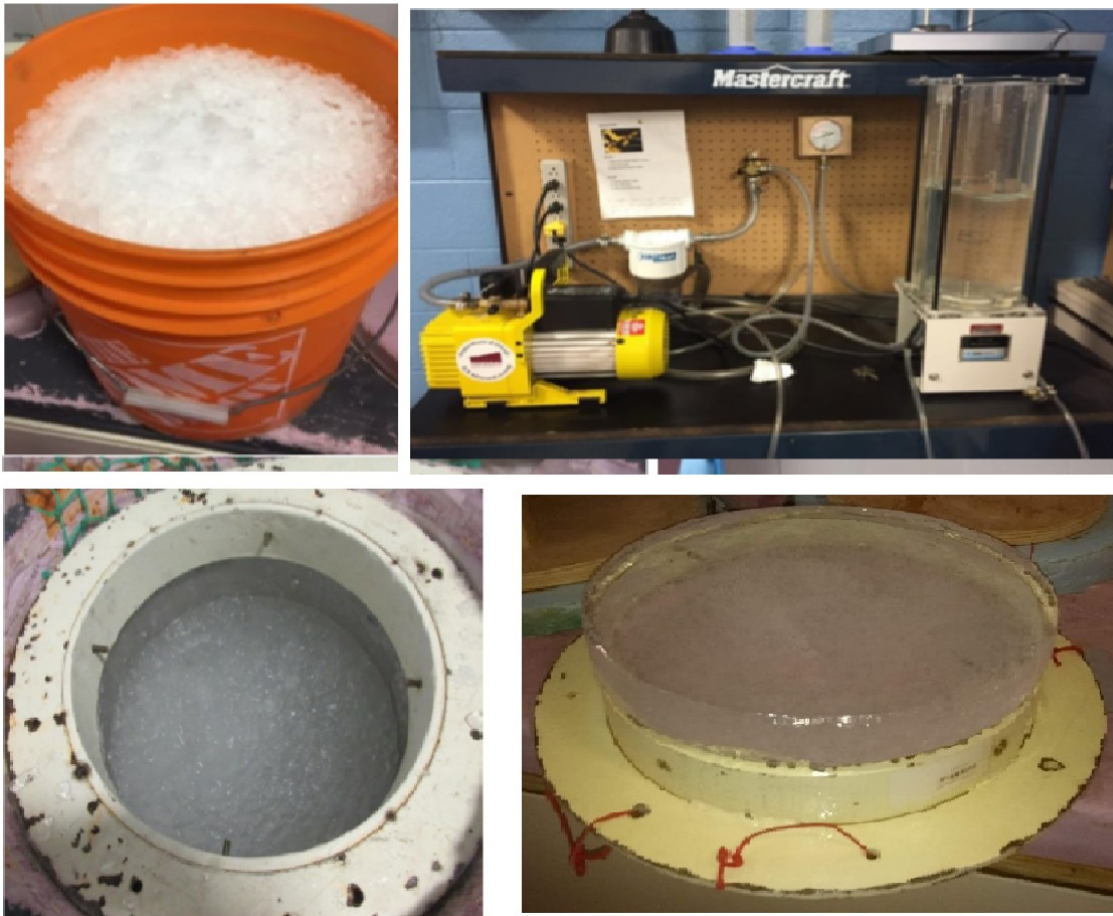


Figure 4.4: Preparation of Ice Sample

Top left: ice cubes were processed in commercial ice chipper, top right: deaeration process of distilled water, bottom left: a metal ring was set inside a mould and filled with the mixture of ice chips and deaerated distilled water, bottom right: The demoulded ice sample shaped using an aluminium plate

To observe the crystal structure of these laboratory-made samples, a thin section of ice was cut and observed under polarized light with a microscope in accordance with the techniques documented in (Bruneau et al., 2013) (Figure 4.6). This shows that the ice was polycrystalline with no preferred orientation, and crystal sizes were approximately 1-6 mm in size.

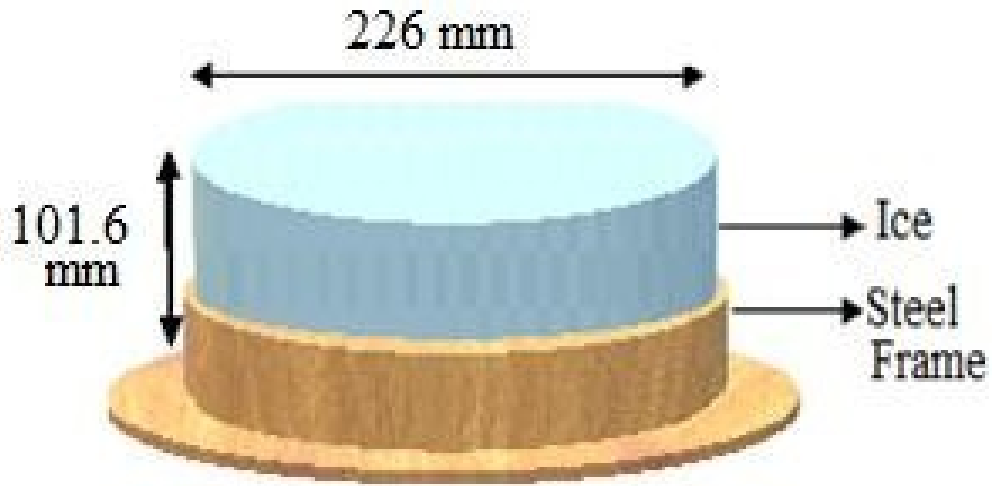


Figure 4.5: Dimension of Ice Sample

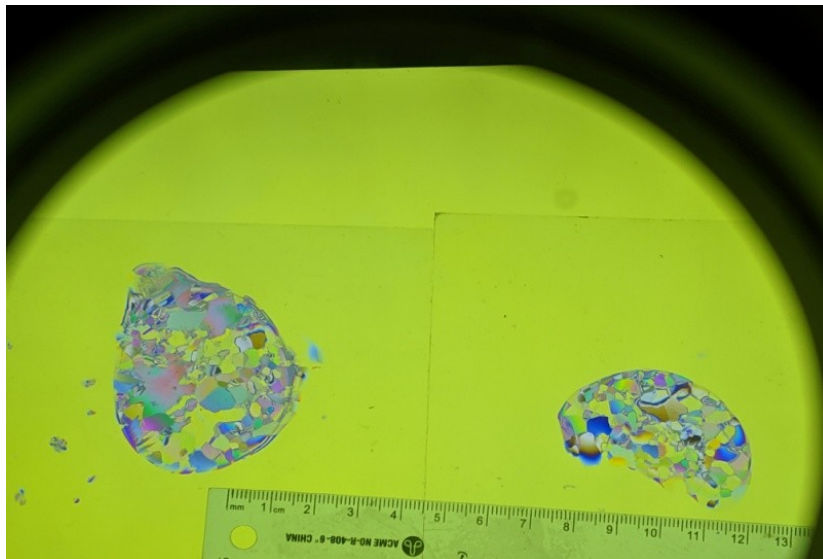


Figure 4.6: Thin Section of Ice Sample

A metal frame was used to clamp the ice sample during the experiment. An aluminum plate was designed to fix the ice specimen and placed over the ice sample upper surface to keep the ice fixed within the metal frame during the experiment (Figure 4.7).

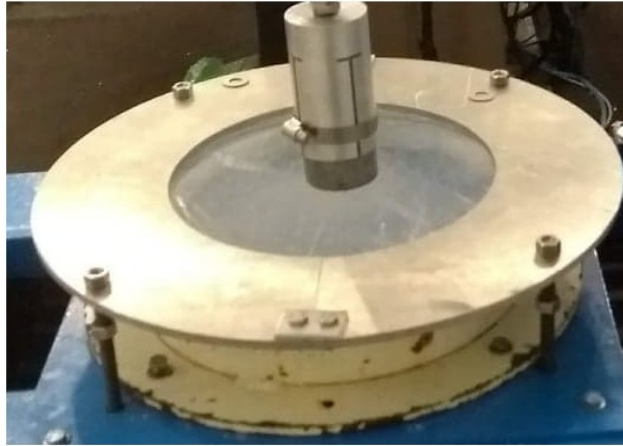


Figure 4.7: Aluminium Plate on the Ice sample to Minimize the Displacement

4.3.2 Concrete Sample

A mid-strength concrete mix was used for this experiment. This type of concrete mix is commonly used in harbor and marina construction. The main reasons for using this mix were,

- The mix provides a consistent sample that can be easily compared with other concrete mixes that may be used for ice interaction experiments
- The mix allows easy reproduction of the same concrete samples or of different samples with the same mix design for other experiments related to ice concrete interaction.

The concrete mix is listed in

Table 4.1. The samples were cast in a cylindrical mould to get cylindrical samples 50.8 mm in diameter and 101.6 mm in height as this is an standard size and shape concrete test sample. These samples were demoulded within 48 hours of casting and kept in curing room to hydrate.

Table 4.1: Concrete mix design for 1 m³

Ingredients	Amount
Cement	400 kg
Coarse aggregate	112.8 kg
Fine Aggregate	94 kg
Water	19.2 kg
Plasticizer	50 ml
Ratios	
Water to Cement Weight Ratio (W/C)	0.4
Coarse Aggregate to Fine Aggregate Volume Ratio (C/F)	1.2

The top and bottom surfaces of each concrete cylinder were cut back with a grinder by approximately the diameter of the fine aggregate to remove the surface concrete and expose the aggregate. The approximate weights of the samples were found to be in the range 435-450 gm before the experiment. The cylinders were individually covered with plastic bags and stored inside the cold room at a fixed temperature before the experiment. Figure 4.8 illustrates the cylindrical concrete sample and the smoothed surface of the specimen.

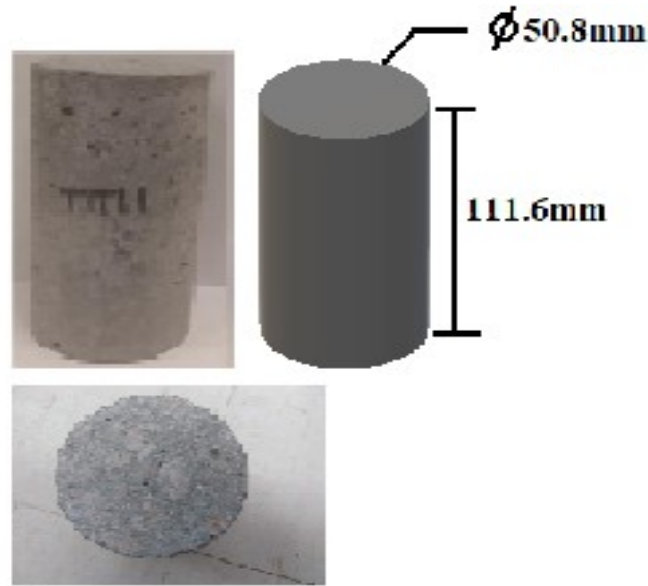


Figure 4.8: Concrete Sample;

Top left; Concrete sample after demoulding; Top right; diagram of concrete sample with dimensions, Bottom; surface of the concrete surface after smoothing in a grinder

For the concrete compressive strength test, six extra samples were cast with dimensions of 4 inches diameter and 8 inches height and tested after 14 and 28 days of casting. The compressive strength was found to be 45 and 50Mpa, respectively at 14 and 28 days. The values are listed in Table 4.2, and the compressive test procedure is illustrated in

Figure 4.9.

Table 4.2: Result of Compressive Test of Concrete after 14 and 28 Days)

Duration After Casting	Compressive Strength of Concrete Cylinder (MPa)			Average Compressive Strength(MPa)
After 14 days	42.23	45.59	47.2	45.01(90%Approximately)
After 28 days	49.68	50.12	51.1	50.3



Figure 4.9: Compressive Strength Testing

4.3.3 Concrete Aggregate Sample

Concrete samples are a combination of cement paste and aggregate which have individual properties. Itoh et al. (1988) conducted abrasion experiments between sea ice and concrete mixes designed with different aggregates. It was found that aggregate can affect the ice concrete abrasion. Although the primary objective here is to obtain the adhesion between the concrete mix and ice, for a more detailed observation, the individual concrete components were also tested separately with ice. These aggregates consist of crushed rock (Figure 4.10), so it was necessary to obtain aggregate rock samples of the same size as the concrete samples in order to fit in the testing apparatus.

A large sample of the aggregate rock (referred to locally as Black Mountain Granite) was obtained from the aggregate manufacturing company. The sample was cored using a drilling machine, usually used in a drilling lab for producing rock samples (Figure 4.11).



Figure 4.10: Aggregate Samples

The sample was expected to be cut in the same dimension of the concrete sample to compare the bond strength easily. However, it was cut to 100 mm height, and 50 mm diameter instead of 50.8 mm diameter as the rock cutter had a limitation for dimension, and this was the nearest dimension to the concrete samples. The top and bottom surface of the rock cylinder was cut flat with the grinder (Figure 4.12).

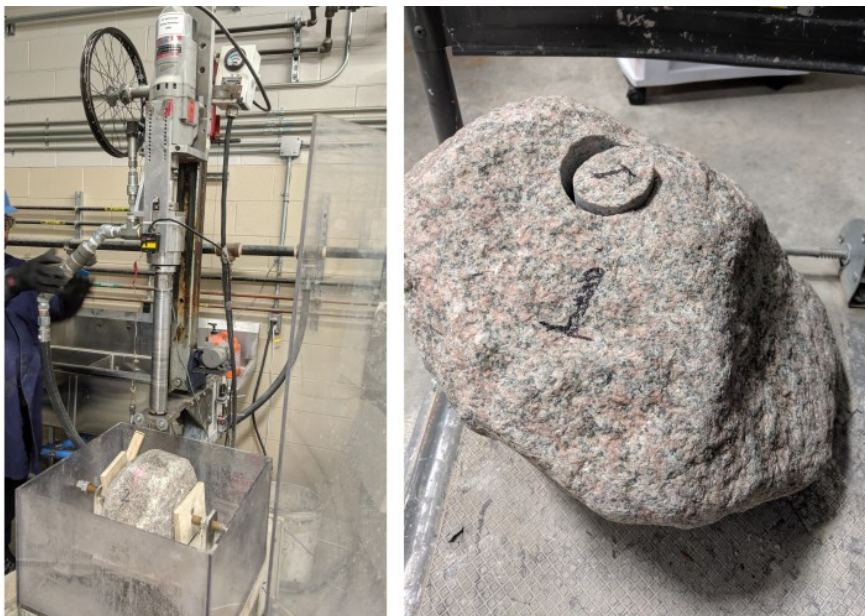


Figure 4.11: Procedure of Cutting Rock Sample

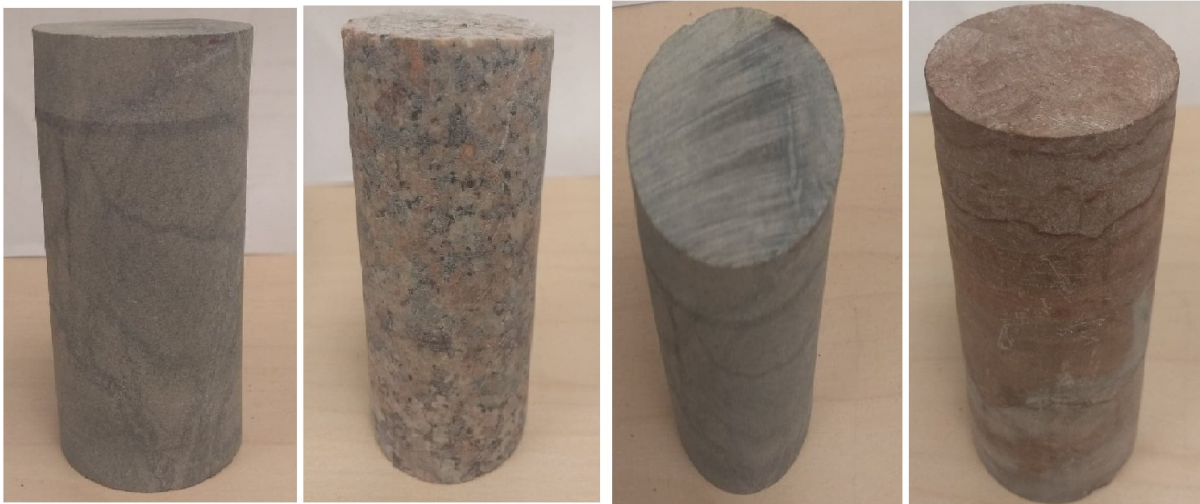


Figure 4.12: Aggregate Testing Samples

4.3.4 Mortar Sample

To compare the adfreeze bond strength between pure mortar paste and the standardized concrete mix, mortar samples were cast with the same dimensions as the concrete samples (50.8mm diameter, 101.6 mm height).

4.4 Instruments and Equipment

Based on the findings of the pilot experiment, the Posi-Test machine was judged to be unsuitable and new apparatus consisting of a purpose-designed lever arm and supporting instruments was designed for the main experimental study.

4.4.1 Lever Arm Apparatus

The main factor driving the re-design of the experiment was the fragility of the bonding for low loads and short durations. During the pilot experiments, the adfreeze bond was found very vulnerable at the initial stage. Thus attaching the pull-off device needed to be conducted very delicately as it had to be done between the applied pressure stage and the pull-off stage and it was found that samples were often dislodged before the bond strength could be measured. Hence a more convenient and robust method was required to apply the contact pressure and then transition to the bond breaking part of the experiment.

A lever arm apparatus was designed to achieve both functions so that the sample did not have to be manipulated during the experiment. The action of gravity provides the steady long-term compressive pressure (illustrated in Figure 4.13). The rationale being that gravitational loading guarantees steady load application regardless of machinery, power systems, displacement of contact surface etc. It is entirely reliable for longer duration tests in which disruption may be expected when using other mechanical systems. The total effective length of the lever arm was 965 mm. The concrete cylinder was inserted in the aluminum holder and the holder attached to the load cell at a certain distance of lever arm (294mm from the hinge).

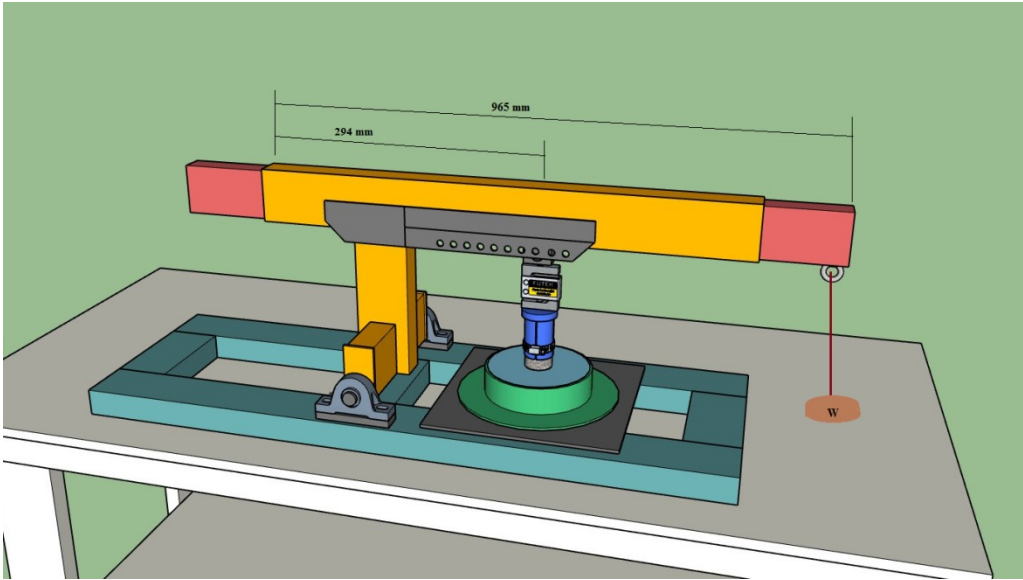


Figure 4.13: Diagram of Lever Arm

A weight bar hangs from a hook at the end of the lever arm to produce the contact pressure on the concrete cylinder. A 1000 lb compression/tension load cell was attached to the concrete sample holder and the resulting data collected with a National Instruments desktop data acquisition computer where the measured load was translated into contact pressure and adfreeze bond strength using NI Labnet software. The important part of the design was to place the load cell as close to the contact point as possible so that the measurement is an unambiguous reading of bond strength and not an inferred reading based on load transmitted

through a mechanical apparatus. The lever apparatus was placed inside the cold room for 24 hours prior to the experiment and for the duration of the experiment. The ice sample was fixed in place by the round metal retaining plate on the top of the sample. The weight bars on the weight pan were changed to apply different contact pressure to the concrete. Before the test, the concrete cylinder was not in contact with the ice surface. At the start of the experiment, the concrete was brought into contact and maintained for a specified period of time by the weight-applied pressure. At the end of the contact duration time, the concrete sample was pulled away from the ice surface by reverse loading to obtain the adhesive bond strength resulting from the contact pressure. A controlled-rate scissor jack was used to gently reverse the loading direction to break the adhesive bond. Measurements were recorded from outside the cold room, using the computer data acquisition system attached to the load cell (Figure 4.14).



Figure 4.14: Experimental Setup

4.4.2 Mechanism and Load Calculation

The contact pressure varies by one of three ways: changing the position of the sample attachment point; changing the length of the telescoping lever arm; and/or changing the weight bars hanging from the lever arm end. Essentially the minimum applied contact pressure results from the self-weight of the fully retracted lever arm and the sample being positioned nearest the lever end. Loads were measured directly at the sample thus it was not necessary to compute them accurately. Thus the actual load measurements and resulting pressures were verified using theoretical calculations.

4.4.3 Aluminium Clamp

An aluminum clamp was designed to hold the concrete cylinder and attach it to the load cell without damaging the sample and to transfer loads uniformly and circumferentially. Eccentric loading might otherwise result in uneven pressures, lateral translation of the sample and damage to the load cell. This aluminum clamp holds the concrete with minimal abrasion to the vertical surface of the cylinder, and is easy to change samples. Aluminum is flexible, and rust-free. One end of the concrete sample was inside the clamp while the other end was exposed to allow the experiment. A threaded rod was used to attach the load cell to the clamp, and a pipe clamp was used to tighten the clamp around the concrete or rock samples during the experiment. The weight of the Aluminium Clamp was 300g approximately (Figure 4.15).



Figure 4.15: Aluminium Holder of Concrete Sample

4.4.4 Box for Submerged Experiment

The submerged experiment was conducted to increase understanding of the ice-concrete adfreeze bond strength under water, compared with the dry test. A watertight metal box was designed (Figure 4.16) whereby the ice sample was fixed inside the box with the original clamping plate. The lever apparatus was able to accommodate the wet test box without any additional modification.

Once the ice sample was fixed inside, the box was filled with the cold water. The temperature of the water was near 0°C. The concrete was not initially in contact with the ice sample and once the box is filled with water, the concrete was then placed on the ice sample following the same method of the dry test.

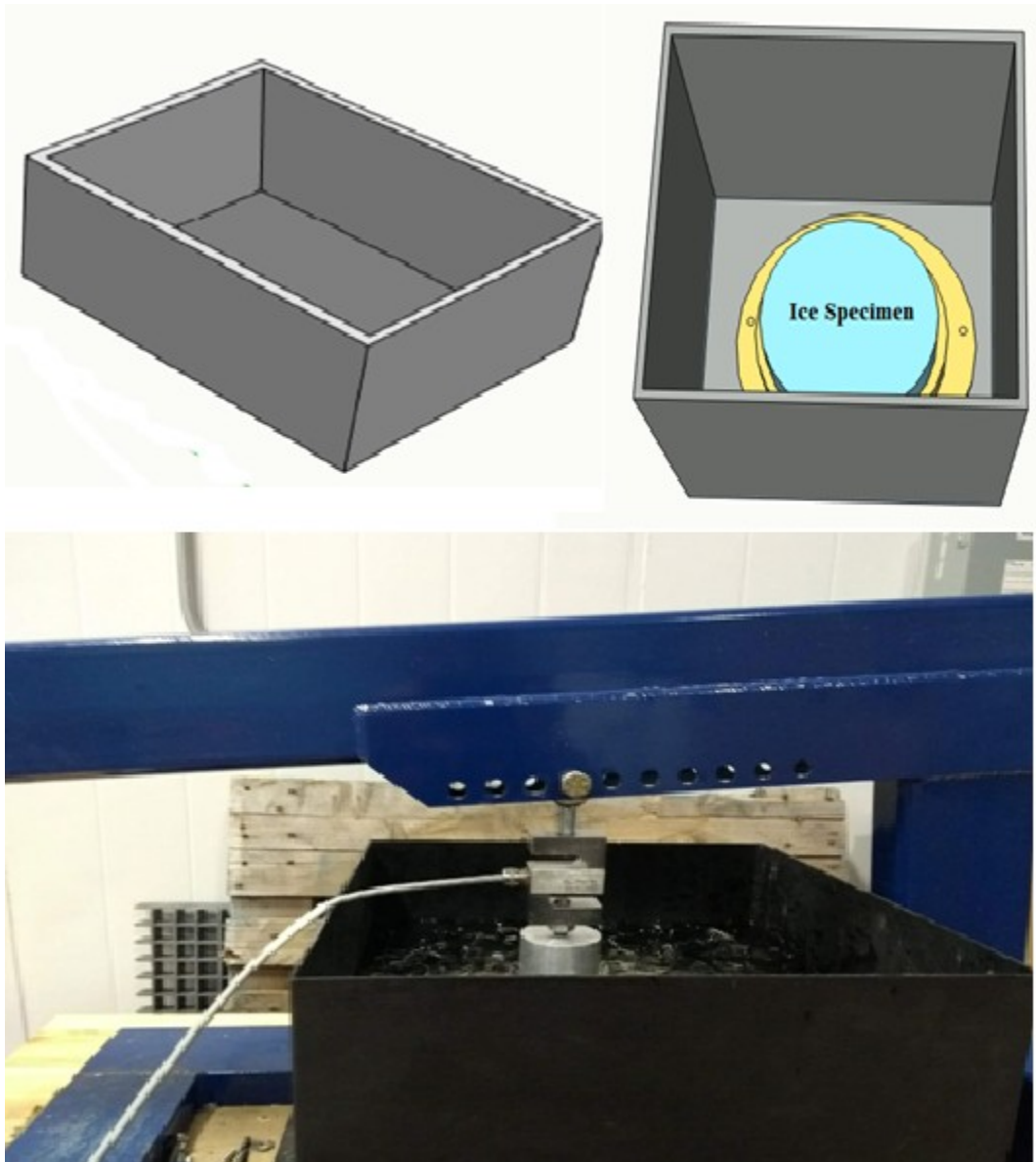


Figure 4.16: Metal Box for Submerged Test

4.4.5 Scissor Jack and Drill

A constant loading was required to operate the lever arm during the experiment. Previous studies have used hydraulic jacks for applied loads. As the current experimental setup scale is smaller than most previous experiments, portable and smaller equipment could be used for load application.

For the current experiment, a scissor jack was used to lower and raise the lever arm. This allowed the sample to be gently lowered to the ice surface with the positive force then applied by the weight when the jack was fully lowered. The jack was then used to lift the lever arm at a pre-set rate in order to apply the separation load. This method did not require any direct interaction with the concrete sample as the jack was placed on the end of the lever arm machine away from the ice concrete interface. Figure 4.17 shows the mechanism of the scissor jack setup.

In order to apply a fixed and constant raising and lowering rate and the resulting loading rate, a hand held electric drill was used. A small metal hook was designed to link the scissor jack thread and the drill. The hook was attached to the scissor jack and operated with a constant rotational rate. An experiment was conducted with the lever arm equipment and drill using a fixed vertical scale indicate that the fixed setting RPM of the drill resulted in a linear displacement rate of 4 mm/s. This was substantially unaffected by load or direction so that a fixed rate of load application and separation was achieved.



Figure 4.17: Mechanism of Scissor Jack

4.5 Dependent and Independent Variables

The range of contact pressure was decided based on the maximum contact pressures reported in the literature, the minimum reasonably achievable with the apparatus and specimen self-weight, the standardized specimen dimensions and the results from the pilot experiments indicating negligible bonding at low pressures. The range of contact durations was selected on the basis of indicators from pilot experiments with less than a minute being impractical to test and showing no bonding, to two hours which represents a reasonable longest tidal stagnation period. Longer tests were performed in the pilot test and might be the focus of future study but University laboratory protocols limited the present study to less than 3 hours.

The cold room temperature, mechanical properties of ice and concrete samples, the surface condition and size of the concrete sample, and the scissor jack velocity (pull-off speed) were fixed for each experiment. The input parameters are listed in Table 4.3. The applied contact pressure value ranged from 112.49-826.41 kPa whereas the time duration of the applied load ranged from 1- 120 minutes. The sole quantitative output is the measured adhesion force which is converted to a pressure and designated as the bond strength.

Table 4.3: Parameters of Experiment

Constant Parameters		
Temperature	-1° C	
Surface area of concrete sample	2025 Area sq mm	
Mechanical property of Ice sample	Replica of natural ice	
Independent Variables with Ranges		
Parameters	Minimum	Maximum
Applied Pressure (kPa)	112	826
Time Duration of applied pressure (Minute)	1	120

4.6 Design of Experiment

The earlier pilot experiments with manual weight application and free standing samples indicated a significant dependence of adhesive bonding with contact pressure and duration. The present experiments were designed to identify these relationships through controlled testing and scientific experimental design.

The experimental test plan was developed as a 7 x 7 matrix in a Latin square method, so the adhesion bond can be observed for each of the time durations under each of the contact pressures including any interaction between independent variables (Table 4.4). Statistical analysis can effectively be conducted with the obtained data set for this test matrix.

The corresponding adhesive force was measured using the load cell – the sample and holder weight having been zeroed out of the raw data set. Three replications were taken for each test, and the average result of the three was used to compute the adhesive pressure.

The same experimental design was followed for both the dry and submerged experiments. The weight of the concrete sample was recorded before and after each test to observe material loss. A photograph was taken before and after for both ice and concrete sample surfaces to observe any changes in abrasion and/or surface damage.

Table 4.4: Experiment Matrix

Contact Pressure (kPa)	Contact Duration (Minute)						
112	1	5	15	30	60	90	120
177	1	5	15	30	60	90	120
264	1	5	15	30	60	90	120
321	1	5	15	30	60	90	120
427	1	5	15	30	60	90	120
585	1	5	15	30	60	90	120
826	1	5	15	30	60	90	120

4.7 Results

The adhesion bond for each experiment was recorded, and the replications are listed in Table 4.5. The average of replications was taken and converted to pressure for further analysis. These results are listed in Table 4.6. It was clearly observed that the adfreeze bond strength increases with the contact pressure and it increases with duration. Likewise, the bond strength is weakened with lower contact pressure and shorter time duration. The results however show considerable variation within the replications suggesting a high natural variability or sensitivity to factors outside experimental control. The variability was highest for lower time duration under low contact pressure. The adhesion strength varied mostly within the range of 112- 321 kPa contact pressure for 1- 15 minutes time duration.

Three replications were taken for each test condition and the average was considered as the final result. For the lower and mid range contact pressure conditions, there were not significant differences among the three replication values for each data point. It was observed that, the replications for adhesion strength were more scattered under higher contact pressure (585 and 826 kPa) and for longer time durations (60-120 minutes).

Table 4.5: All trials: Adhesion Strength (N) between ice and concrete with varying force and duration under constant temperature (-1° C)

Applied Force (N)	Contact Duration (Minute)													
	1		5		15		30		60		90		120	
	Adhesion Force (N)													
228	Trial 1	0	Trial 1	0	Trial 1	2.4	Trial 1	2.66	Trial 1	3.03	Trial 1	3.05	Trial 1	5.22
	Trial 2	0	Trial 2	0	Trial 2	2.36	Trial 2	2.67	Trial 2	2.76	Trial 2	2.69	Trial 2	5.18
	Trial 3	0	Trial 3	0	Trial 3	2.59	Trial 3	2.71	Trial 3	2.49	Trial 3	2.66	Trial 3	5.089
358	Trial 1	1.1	Trial 1	1.38	Trial 1	2.65	Trial 1	2.86	Trial 1	2.97	Trial 1	3.3	Trial 1	5.95
	Trial 2	1.4	Trial 2	1.27	Trial 2	2.54	Trial 2	2.79	Trial 2	2.72	Trial 2	2.81	Trial 2	6.19
	Trial 3	1.16	Trial 3	1.25	Trial 3	2.63	Trial 3	2.66	Trial 3	3.07	Trial 3	2.98	Trial 3	6.13
535	Trial 1	1.65	Trial 1	1.57	Trial 1	2.83	Trial 1	2.5	Trial 1	3.03	Trial 1	3.9	Trial 1	5.95
	Trial 2	1.4	Trial 2	1.42	Trial 2	2.76	Trial 2	3.3	Trial 2	2.7	Trial 2	3.8	Trial 2	6.65
	Trial 3	1.75	Trial 3	1.21	Trial 3	2.3	Trial 3	3.08	Trial 3	4.1	Trial 3	2.74	Trial 3	7.41
650	Trial 1	1.11	Trial 1	1.64	Trial 1	3.08	Trial 1	2.98	Trial 1	4.18	Trial 1	4.05	Trial 1	8.32
	Trial 2	1.47	Trial 2	1.52	Trial 2	2.91	Trial 2	3.17	Trial 2	3.07	Trial 2	5.9	Trial 2	7.9
	Trial 3	1.29	Trial 3	1.34	Trial 3	2.9	Trial 3	3.48	Trial 3	3.43	Trial 3		Trial 3	8.08
865	Trial 1	1.55	Trial 1	1.58	Trial 1	3.82	Trial 1	4.49	Trial 1	5.85	Trial 1	9.9	Trial 1	8.6
	Trial 2	0.94	Trial 2	1.52	Trial 2	3.91	Trial 2	4.1	Trial 2	6.19	Trial 2	10.6	Trial 2	11.2
	Trial 3	1.23	Trial 3	1.55	Trial 3	3.97	Trial 3	3.99	Trial 3	6.21	Trial 3	7.61	Trial 3	12.48
1186	Trial 1	1.34	Trial 1	2.5	Trial 1	7.39	Trial 1	10.43	Trial 1	10.72	Trial 1	15.1	Trial 1	18.79
	Trial 2	1.05	Trial 2	1.08	Trial 2	7.92	Trial 2	8.49	Trial 2	11.9	Trial 2	13.89	Trial 2	
	Trial 3	1.64	Trial 3	2.9	Trial 3	8.33	Trial 3	6.03	Trial 3	11.06	Trial 3	14.51	Trial 3	
1675	Trial 1	1.43	Trial 1	1.5	Trial 1	7.38	Trial 1	6.95	Trial 1	12.5	Trial 1	18.6	Trial 1	24
	Trial 2	1.78	Trial 2	2.17	Trial 2	10.08	Trial 2	14.2	Trial 2	10.4	Trial 2	17.6	Trial 2	22.2
	Trial 3	1.62	Trial 3		Trial 3	8.73	Trial 3	10.575	Trial 3	10.95	Trial 3	19.1	Trial 3	25.5

Table 4.6: Average Adhesion Strength (kPa) between ice and concrete at varying pressure and duration under constant temperature (-1° C)

Contact Pressure (kPa)	Contact Duration(Min)						
	1	5	15	30	60	90	120
112	0	0	1.21	1.32	1.36	1.38	2.62
177	0.6	0.64	1.29	1.37	1.44	1.51	3.01
264	0.79	0.69	1.35	1.46	1.61	1.73	3.29
321	0.64	0.74	1.46	1.58	1.76	2.48	4.0
427	0.61	0.77	1.97	2.07	3	5.66	8.79
585	0.66	0.89	3.89	4.01	5.54	7.15	9.28
826	00.82	0.91	5.49	5.55	7.29	9.13	11.84

The maximum adhesion bond was observed to be 11.84 kPa under a contact pressure of 826.41 kPa for 120 minutes duration. A significant adfreeze bond was observed even at shorter durations when the experiment was conducted at higher contact pressure.

There was no bond strength observed at contact pressures less than 112.49 kPa within 5 minutes duration. The minimum bond strength was measured at 1.20 kPa after 15 minutes of duration at 112.49 kPa contact pressure. This contact pressure is the self-weight of the concrete sample (463gm approximately), and no external contact pressure was applied in this case. When the applied contact pressure is a bit higher, that is 176.63 kPa, an adfreeze bond was observed even after 1 minute of duration, which is 0.60kPa.

The collected data is plotted in Figure 4.18 with contact duration(s) on the x-axis and ice concrete bond strength (kPa) on the Y axis. Each of these series shows the increasing trend of adhesion strength with increasing applied pressure and contact duration. For higher applied pressure such as 826.41 kPa, 585kPa, and 426 kPa, the adhesion strength is observed from 1-

minute time duration and rapidly increases after 5 minutes. The adhesion strength moderately increases for 15-30 minutes, and in some cases up to 60 minutes, it starts to increase more rapidly after that time point.

The adhesion strength was comparatively weaker for the lower applied pressures, such as 112.49, 176.63, 263.95, 320.69 kPa. It also starts to increase after 5 minutes of contact duration but tended to remain linear up to 15-90 minutes of duration. A significant increase was found at 120 minutes of duration. For these applied pressures, there is an overlap found in the adfreeze bond strength at the initial durations, such as 1 or 5 minutes. The bond strength values are not different from each other, although, for higher applied pressure, the bond strengths are quite different from the shorter time duration (Figure 4.18).

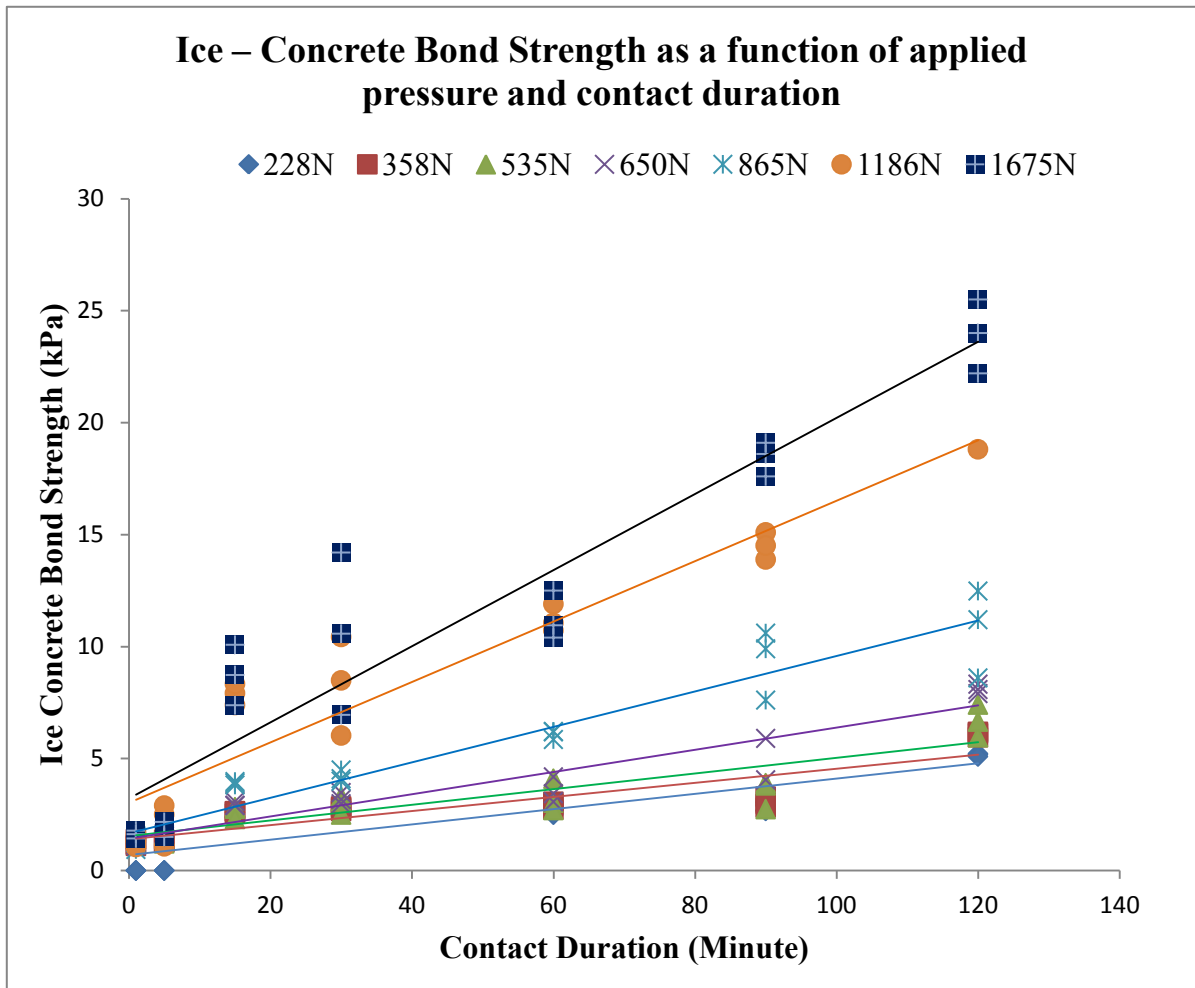


Figure 4.18: Ice-Concrete Adhesion Pressure versus Contact Duration at Various Normal Stresses

4.8 Analysis

The data of Figure 4.18 was analyzed using multiple regression analysis. An ANOVA test was used to statistically assess the impact of applied pressure, contact duration, on the adhesion strength and determine if the test results are statistically significant.

The ANOVA outputs are listed in Table 4.7 and the fit plot of this analysis shows in Figure 4.19 and Figure 4.20. As the F value is less than 0.05, the trends in the data set are shown to be statistically significant for a linear fit in both variables.

Table 4.7: Multiple Regression Analysis of Collected Data

ANOVA								
	df	SS	MS	F	Significance F			
Regression	2	2.82E+08	1.41E+08	73.65	4.56E-15			
Residual	46	87989885	1912824					
Total	48	3.7E+08						
	Coefficients	Standard Error	t Stat	P-value	Lower 95%	Upper 95%	Lower 95.0%	Upper 95.0%
Intercept	-1868.07	441.41	-4.23	0.000	-2756.59	979.55	-2756	979.55
Normal Pressure	7.154326	0.85	8.35	8.78E-11	5.43	8.87	5.43	8.87
Duration	41.09	4.66	8.79	2.02E-11	31.69	50.49	31.69	50.49

The fit could be improved by conducting the regression analysis using a single independent variable derived by combining the two independent variables. The single variable was named Contact Persistence, and the output was the same as before, that is adhesion strength.

$$\text{Contact Persistence} = \text{Pressure} \times (\text{Time}^{0.5}) \quad \mathbf{4.1}$$

Under the contact pressure of 112.49 kPa with 30 minute time duration, the contact persistence will be

$$112.49 \times (30^{0.5}) = 616. \text{ kPa} - \text{sec}^{1/2}$$

This data set is listed in Table 4.8.

Table 4.8: Contact Persistence and Corresponding Adhesion Strength

Contact "Persistence" kPa-sec^{1/2} (Pressure x Time^{0.5})	Adhesion Strength Pa	Contact "Persistence" kPa- (Pressure x Time^{0.5})	Adhesion Strength Pa	Contact "Persistence" kPa-sec^{1/2} (Pressure x Time^{0.5})	Adhesion Strength Pa
112	0	1445	1460	4048	5664
251	0	2044	1613	1460	8792
435	1208	2504	1726	1613	661
616	1322	2891	3290	1726	888
871	1361	320	636	3290	3887
1067	1381	717	740	636	4008
1232	2614	1242	1455	740	5535
176	601	1756	1583	1455	7154
394	641	2484	1756	1583	9280
684	1287	3042	2477	1756	819
967	1366	3512	3996	2477	912
1368	1440	426	611	3996	5485
1675	1504	954	764	611	5552
1934	3004	1652	1968	764	7293
263	789	2337	2067	1968	9127
590	690	3305	3002	2067	11841
1022	1351	-	-	-	-

A new regression analysis was done using the data set of Table 4.9: Statistical Analysis of Contact Persistence and Adhesion Strength (output in 4.9). The F value is less than 0.05 so this set of data is statistically significant. Also the summary of regression analysis is compared in 4.10; comparing both linear and multiple regression analysis, there is a significant difference observed between the values of R for the two methods.

Table 4.9: Statistical Analysis of Contact Persistence and Adhesion Strength

ANOVA						
	df	SS	MS	F	Significance F	
Regression	1	33	33	521.61	4.34E-27	
Residual	47	30565277	650325.05			
Total	48	369782187				
	Coefficient s	Standard Error	t Stat	P-value	Lower 95%	Upper 95%
Intercept	-97.23	170.97	-0.56	0.57	-441.19	246.73
Contact Persistence	1.27	0.055	22.83	4.34	1.16	1.39

Table 4.10: Comparison between Regression Output of Original Data and Contact Persistence

Regression Statistics		
	Original Data	Contact Persistence
Multiple R	0.872954435	0.957779976
R Square	0.762049445	0.917342483
Adjusted R Square	0.751703769	0.915583813
Standard Error	1383.04866	806.4273374
Observations	49	49

The normal probability plot of two regression analysis was illustrated (Figure 4.19 and Figure 4.20) with sample percentile on x axis and adhesion strength on y axis. There is no discernible difference found between these probability plots. However based on the improvement in correlation (R) the analysis using the Contact Persistence variable was used to generate a predictive equation.

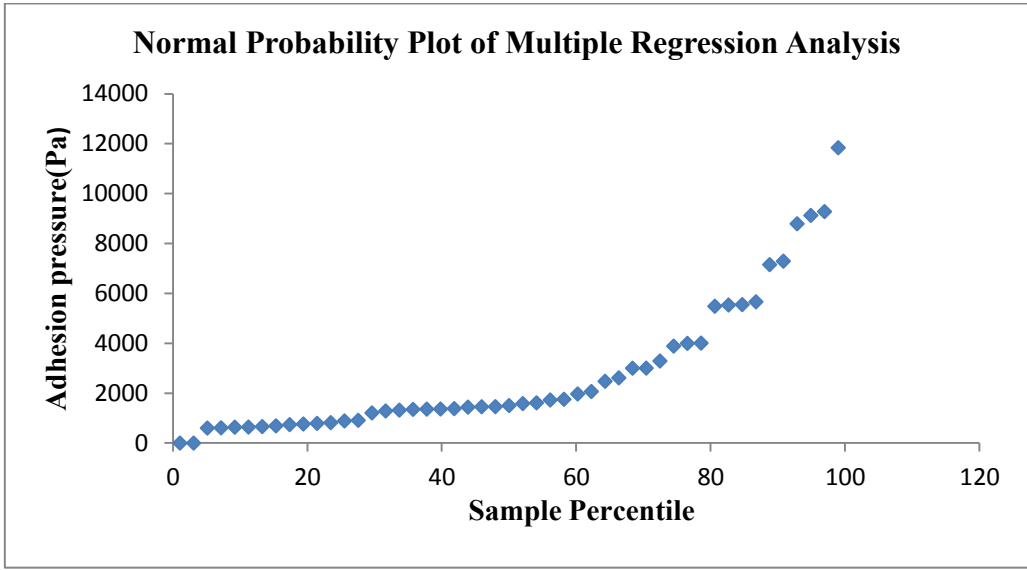


Figure 4.19: Normal Probability Plot of Multiple Regression Analysis

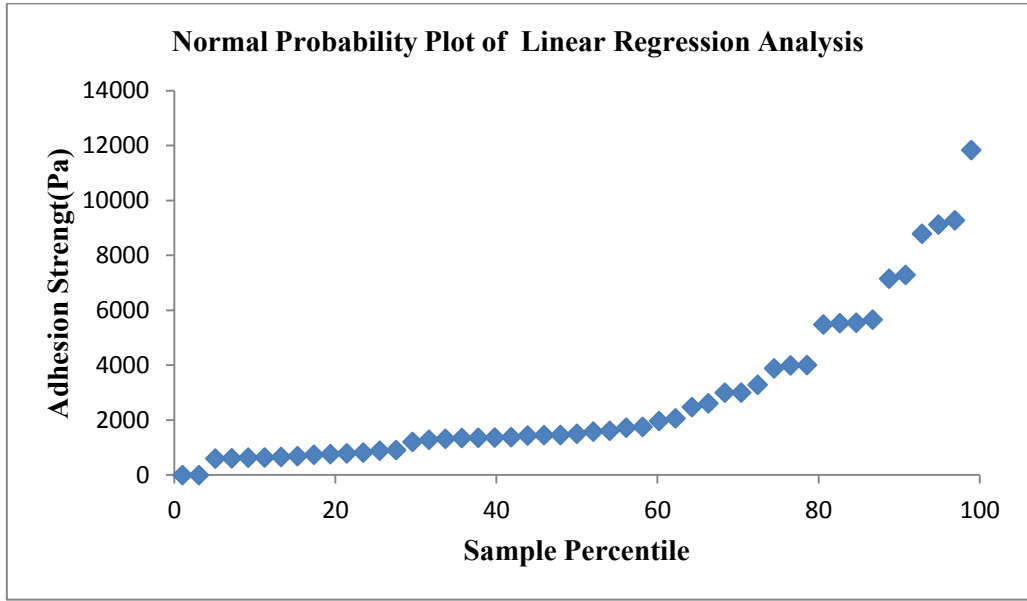


Figure 4.20: Normal Probability Plot of Linear Regression Analysis

Predicted values of adhesion strength were obtained from the regression analysis using the Contact Persistence approach. To compare the predicted and measured results, a fitted curve was plotted for each contact pressure. Figure 4.21, Figure 4.22, Figure 4.23, illustrate the comparison between the regression and measured values of the adhesion strength with the

duration on the x-axis and adhesion strength on the y-axis. The fitted curves for the entire 7x7 matrix are plotted in Figure 4.24 with the duration on x-axis and contact pressure on y-axis.

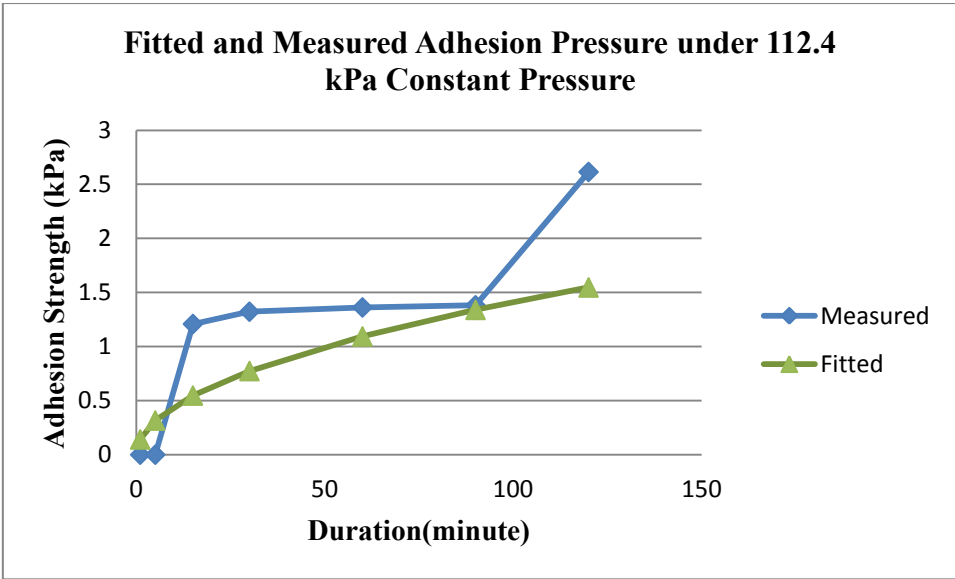


Figure 4.21: Fitted Curve of Adhesion Strength under 112.49 kPa Contact Pressure

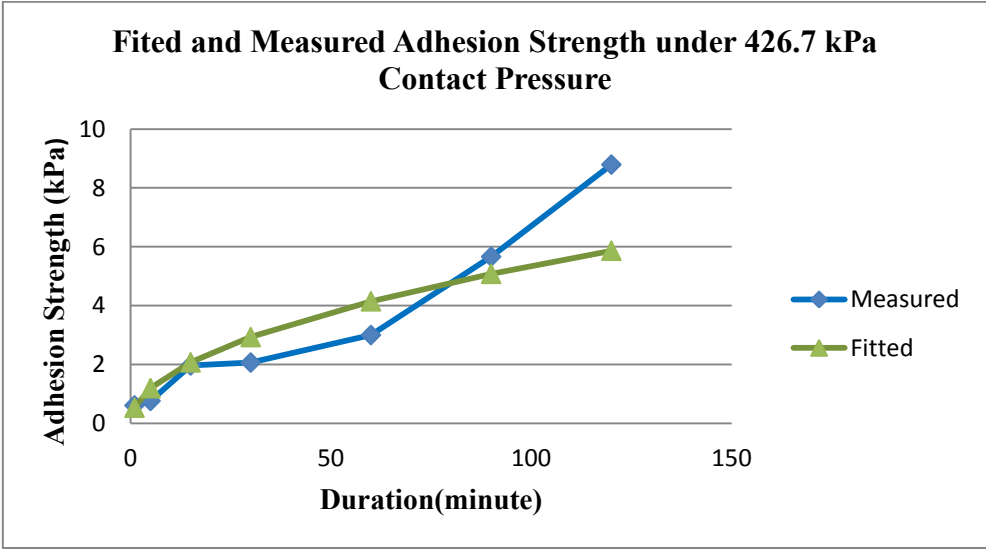


Figure 4.22: Fitted Curve of Adhesion Strength under 426.7 kPa Contact Pressure

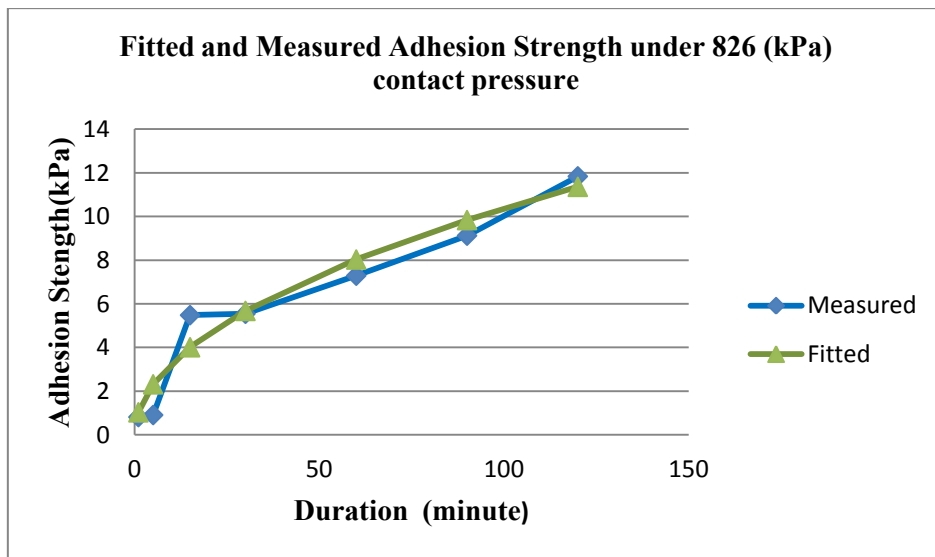


Figure 4.23: Fitted Curve of Adhesion Strength under 826 kPa Contact Pressure

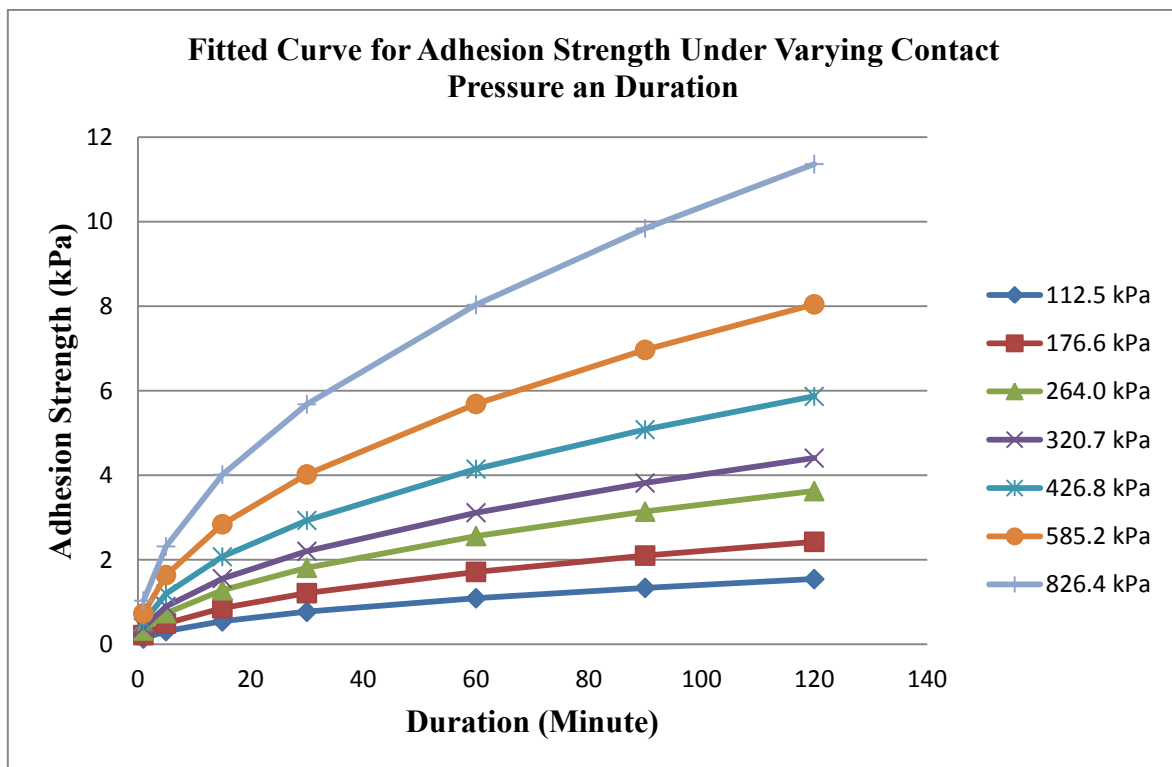


Figure 4.24: Fitted Curve of Adhesion Strength under Varying Pressure and Duration

These plots show that the agreement between regression and measured values is poor for the low pressure data and improves as the applied pressure increases.

4.8.1 Data Validation

Contact Persistence was calculated using the data set from Table 4.8. The data was plotted in Figure 4.25 with contact persistence on x axis and adhesion strength on y axis. A trend line was fitted in the scattered data set and the equation was found

$y = 1.2551x$

4.2

Where,
 y= Adhesion Strength
 x= Contact Persistence

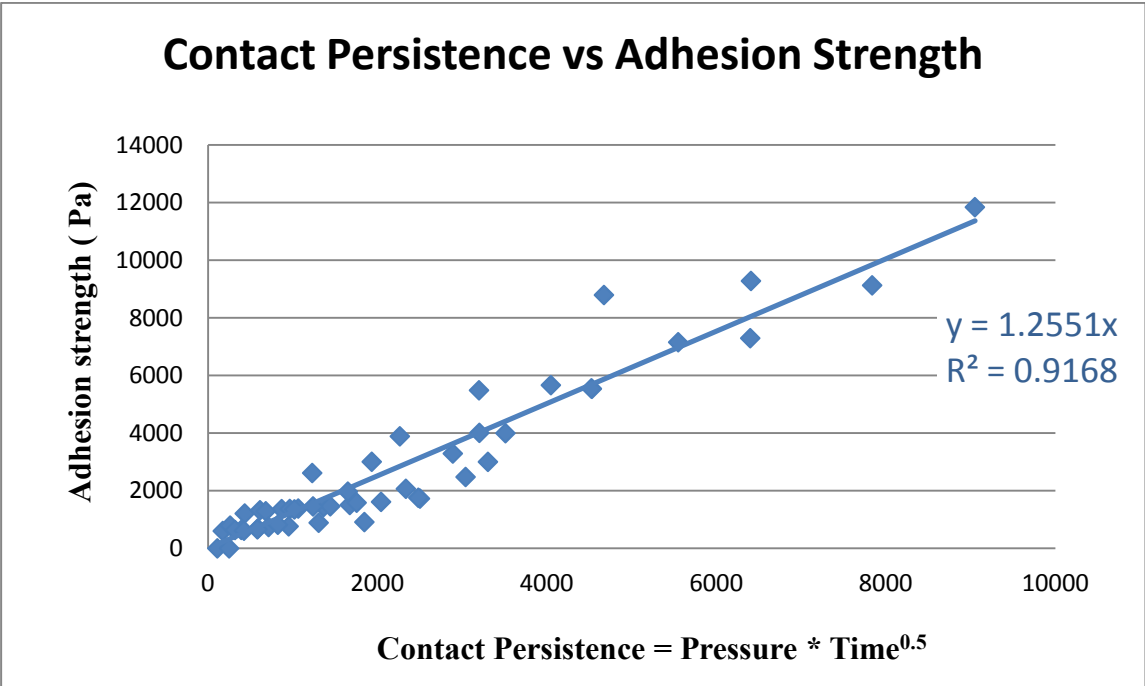


Figure 4.25: Contact Persistence vs Adhesion Strength

Two previous tests from the pilot experiment, which had not been included in the data analysis, were used to further test the Persistence variable analysis. For the first case, the independent variables were within the range of the current experimental data set 512 kPa contact pressure for 30 minutes time duration. For the second case, the duration was within the range (120minutes), but the contact pressure of 970 kPa was beyond the range of the analyzed data contact pressure.

For both cases adhesion strength was calculated using Equation 4.4. The predicted and measured outputs are listed in Table 4.11.

Table 4.11: Comparison of Theoretical and Practical Output

Contact Pressure (kPa)	Duration (min)	Adhesion Strength(kPa)		Error (a-b) kPpa
		Regression Output using Equation 4-4(a)	Measured Output From Laboratory (b)	
512	30	3.51	4.59	1.3 (28%)
970	120	13.33	17.18	3.8 (22%)

Figure 4.11 shows that the theoretical and practical value of the adhesion strength under two different applied pressure and contact duration. The differences are comparable within about 25%.

4.9 Material Loss and Findings

The series of experiment results showed measurable material loss for both ice and concrete samples. These abrasion effects were found to be clearly dependent on the contact pressure and duration.

4.9.1 Concrete Material Loss

The concrete sample weight was recorded before and after each test. As the experiment was designed at a very small scale, a measurable material loss was not observed each time. The same concrete sample was used for the series of experiments in order to find the gross material loss. After multiple tests a measurable material loss was observed in the concrete surface. Also the weight of the concrete sample was reduced after a number of tests when compared with the initial weight of the concrete sample before the entire experiment. The initial weight of the concrete sample was 463 gm before the experiment and the final weight was observed 450.5gm after series of tests. In addition photographs were taken after each test.

The progressive changes of the concrete surface were quite clear when observed directly by eye but it was difficult to take clear photograph due to the dark shade of the concrete specimen. Figure 4.26 shows the material loss from the concrete surface.



Figure 4.26: Surface Material Loss of Concrete Sample after Series of Experiments

4.9.2 Ice Indentation and Loss of Ice Surface

A clear indentation was observed on the ice sample surface after nearly every test. The indentation was deeper for higher contact pressures and longer time durations. The indentation was not prominent for the lower contact pressures, but for the higher contact pressure there was clear material loss observed on the ice surface. Ice was found sticking to the concrete surface after pulling the sample apart from the ice and concrete particles were observed on the ice surface. Photographs were taken of the ice surfaces, with one example in Figure 4.27.

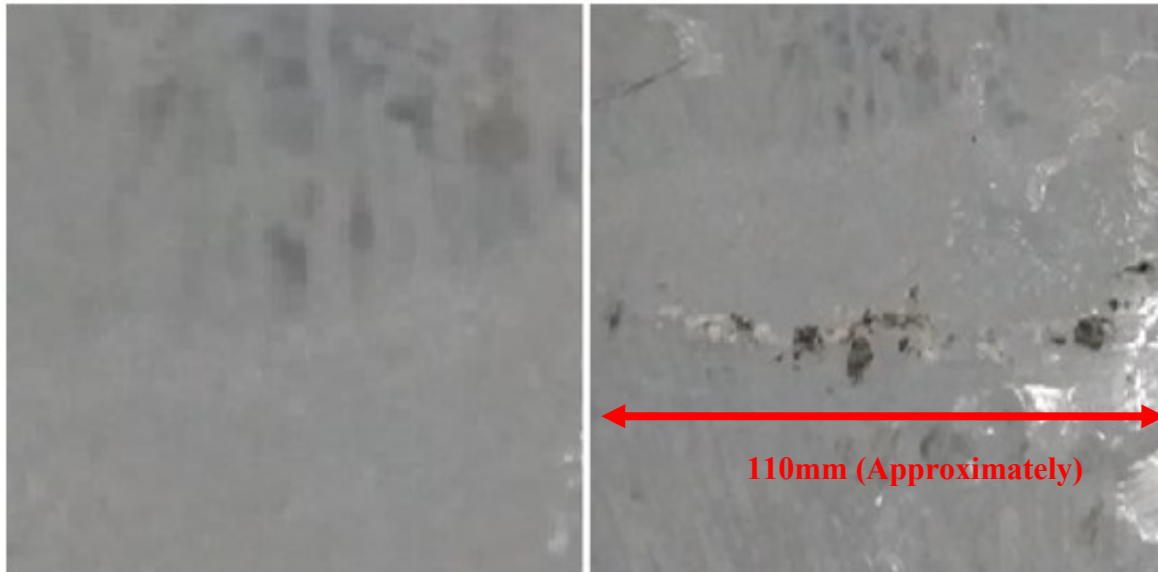


Figure 4.27: Ice Surface before and after the Experiment with Abraded Concrete Particles

4.9.3 Ice Adhesion over Aggregate

Some Ice was found sticking to the concrete surface, for almost every experiment. Depending on the contact pressure or duration, the ice pieces were larger or smaller Figure 4.28. It was a thin layer for lower contact pressure such as 112.49 or 176.63 kPa whereas a significant amount of ice was observed for 826.41 kPa after 120 minutes duration. As the concrete specimen was smoothed prior to testing, the aggregates are exposed on the ice surface. In general the maximum ice particles were found to be sticking to the areas where the aggregate surface was exposed. To observe this in more detail, a thin line was drawn over the border of that particular aggregate and after the experiment, a piece of ice was obtained sticking over the marked area This finding led to an extension of the experiment with an aggregate stone sample to observe the adhesion property of the aggregate and concrete paste separately.



Figure 4.28: Ice Piece Sticking to the Concrete Surface after the Experiment

4.10 Submerged Experiment

In real life, marine structures are always partially submerged in water. That is, the structures are exposed to ice collision for both dry and submerged conditions. To compare the adhesion bond and corresponding ice abrasion, a submerged test was planned to be conducted with the same test matrix as the dry tests. The ice cylinder was fixed inside a water bath filled with distilled water. The water temperature was near 0°C. Ice cubes made of the same distilled water were added to the water to maintain the temperature of the water for the long time duration tests.

The entire test was planned to be conducted at an ambient air temperature of 1 °C inside the cold room. The temperature was higher than the dry test to prevent the water from freezing. All the equipment and samples were put inside the cold room 12 hours prior to the experiment except the ice cylinder. The ice cylinder was stored separately at -1°C to avoid melting. The concrete cylinder was attached to the load cell and lever arm and was not in contact with water prior to the experiment. Once the box was filled with water, and the ice sample was completely submerged, the concrete sample was placed in contact with the ice sample using

the same procedure, used for the dry test. Almost 80% of the concrete cylinder was under water except for the upper part. The upper part was attached to the load cell, and water contact was avoided to prevent damage to the load cell (Figure 4.29).

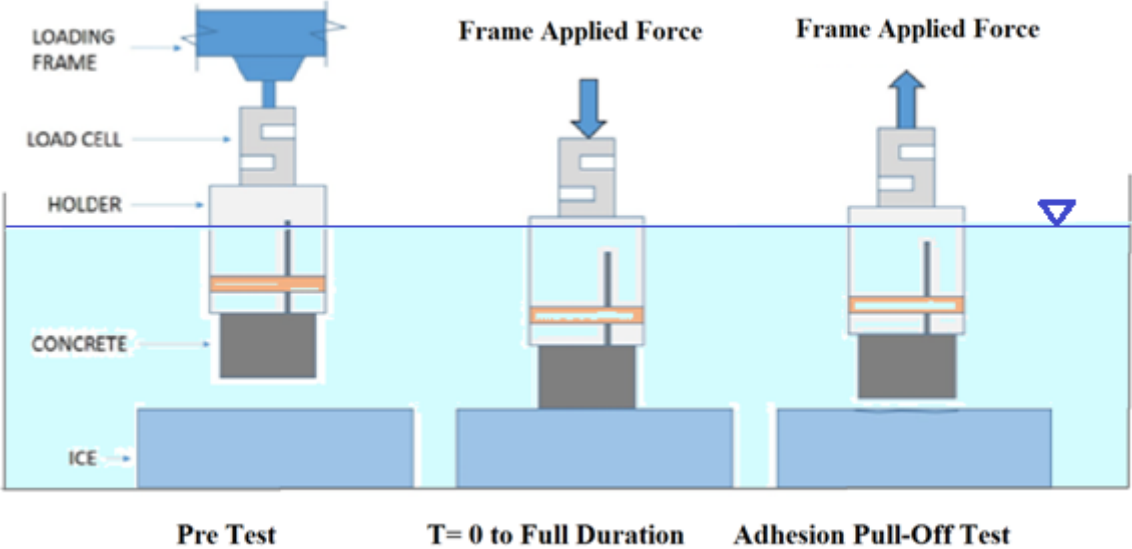


Figure 4.29: Mechanism of Submerged Experiment

These tests were interrupted after a brief initial trial by the onset of the COVID-19 Pandemic and the resulting closure of the University. In the initial trial experiment the adhesion bond was found to be significantly higher in the wet tests than for the corresponding conditions of the dry test, and the ice material loss for the ice sample was also more significant than the dry test. The experiment was conducted on a small scale, thus the abrasion to the concrete sample could not be measured as the concrete particles were dissipated in the water, but the ice sample loss was clearly observed. Also the concrete sample absorbed some amount of water when it was submerged during the test. So recording the weight of concrete before and after test was also not an appropriate method to measure the concrete loss. A good amount of ice was found sticking on the concrete surface after pulling the concrete specimen away from the ice (Figure 4.30).The ice surface condition was not accurately observed as the sample was

under the water, and the temperature was above the freezing point. When the box was drained, the ice surface was already melted, and the evidence of material loss was not prominent. However, the ice material loss is evident from the quantity of ice sticking onto the concrete sample.



Figure 4.30: Ice Piece Sticking on to the Concrete Surface after the Submerged Test

In this experiment, the concrete particles could not be measured as the amount of concrete abrasion was small compared to the amount of water. For a larger scale of experiment, the water can be filtered through a paper filter, which can trap the micro fine particles of abraded concrete, and the abrasion can be measured in detail. Also it was hard to conduct experiments for longer time durations, as the ice sample starts to melt with longer times and separates from the metal frame retainer. Once the ice was no longer tightly attached inside the frame, the experiment was difficult to conduct as the ice moves under the action of the pull-off force acting on the concrete sample. For the submerged test, with 60 minutes contact duration under 265.95 kPa applied pressure, the adhesion strength was observed to be 18.8 kPa, whereas for the dry test, with the same contact duration and applied pressure, the adhesion strength was observed 1.61 kPa. It is highly recommended that these experiments be conducted in the

future to conclude the submerged analysis relative to the dry tests using the same laboratory setup.

Chapter 5 Discussion and Conclusions

This chapter discusses the significant findings and conclusions of the pilot and refined experiments. Though the adhesion strength can be theoretically defined, the experimental findings of adfreeze bond strength and failure may vary from the theoretical. Limitations of this work and recommendations for future work are detailed in the next chapter.

5.1 Experimental Findings and Discussion

The experiment was conducted with variable pressure and duration under a fixed temperature of -1°C to measure adhesion strength between ice and concrete with corresponding concrete abrasion. A nonlinear relationship was observed from the test results, and the adhesion strength of the ice was found directly proportional to the contact pressure and non-linearly proportional to applied pressure duration. The adfreeze bond strengths were higher with higher contact pressure and duration and lower under shorter duration with lower contact pressure for both dry and submerged experiments.

As previously discussed in Chapter 2, the adhesion strength depends on the rigidity of surface, temperature and surface roughness. In the current study, the concrete sample was reasonably rigid, and the ice specimen was relatively warm. During the experiment, ice material loss was found almost after every test, which can be considered as a brittle failure.

In the current study, the pilot experiment has shown that the adfreeze bond is weaker at lower temperatures. Although the experiment was conducted at -1°C (near 0°C), the ice and concrete were completely dry before the experiment. There is a chance that a water film might not be significant in the ice concrete interface but it is more likely that some liquid was available at the interface due to the relatively warm temperature. This would be a feature of most realistic ice interaction scenarios. This liquid also probably improves the bond formation.

5.1.1 Contact Persistence

The adhesion strength was observed for different contact pressure and duration and multiple regression analysis was conducted with the obtained data. Besides this, a linear regression analysis was also conducted where the two variables contact duration and contact pressure were converted into one variable that is contact persistence ($\text{Pressure} \times \text{Time}^{0.5}$) with the same output. There was no significant differences found between the normal probability graphs of this two different regression analysis but the fit plot was found to be more accurate in the regression analysis. As the adhesion strength remained same for both and the normal probability plot was also not different, the result of linear regression analysis was considered as the final output.

5.1.2 Ice Concrete Interface

The concrete surface is quite rough on the microscopic scale and it has many micro-pores. As the same concrete sample was used here for a dry test, there is a good chance that water droplets were frozen inside the concrete sample for a longer duration. When the submerged experiment was conducted, instead of the regular indentation, a significant amount of ice specimen was broken when the concrete sample was pulled away. The presence of water at the ice concrete interface generates partial failure instead of pure adhesion failure.

5.1.3 Concrete Abrasion

The weight of the concrete cylinder was measured each time before and after the experiment. However, after a series of experiments, the material loss was found to be 12 gm (approximately) after 147 experiments (that is 7x7 series of experiments with three replications). The average loss per experiment was 0.816 gm.

It was found that there is a failure in the ice sample under higher pressure and longer duration. Instead of concrete abrasion, the material loss was observed in the ice sample. So the adhesion bond might be higher under higher contact pressure and duration, but it does not

typically indicate a higher abrasion mechanism. As the scale of the experiment was comparatively small to measure the concrete abrasion, it was intended to measure the concrete surface roughness using a laser scanner to compare the concrete surface before and after the experiment. This was also not possible due to the pandemic situation.

5.1.4 Adhesion to Aggregate

During some experiments, more significant ice adhesion was observed over areas of exposed aggregate. It was postulated that the aggregate might have higher adhesion with ice compared to other components of the concrete. As the ice adhesion largely depends on the surface roughness, rigidity, and the porosity, there is a chance that the particular aggregate satisfies one or all of these parameters. To compare the adhesion strength individually, aggregate rock samples and cement paste samples were prepared to test under the same contact durations and applied pressures used for the regular concrete samples. Due to COVID-19 situation, these experiments were not possible to conduct.

5.1 Summary

This study was designed to investigate the ice concrete adhesion bond strength and corresponding concrete abrasion. The main objective of this study was to measure the strength of the ice-concrete adhesion bond as a function of applied pressure and the time duration of the applied pressure. A second objective was to measure the loss of concrete material at the interface when the bond was broken.

At first, a literature survey was done with the prior studies of ice concrete adhesion. Based on the previous studies, the critical parameters were considered, and an experimental study was designed to measure adhesion bond strength between freshwater ice and mid-strength concrete with various contact pressure and duration under a constant temperature of -1°C . The experiments were conducted for both dry and (one) submerged tests.

A pilot experiment was conducted, and then the test setup was improved. A nonlinear relationship was found for adhesion strength with various contact pressure and duration. The laboratory obtained data set was statistically analyzed and validated using an equation derived from the raw data set. A single submerged test was also conducted, and the adhesion was observed to be higher than the corresponding dry test. The experiment was conducted on a small scale, so there was not much concrete abrasion observed. Photographs, taken before and after each experiment, show the abraded concrete particles and indentation over the ice surface. Also the average concrete abrasion rate was found to be low on average for each test.

Chapter 6 Limitations and Recommendations

This chapter describes the limitations of the current work and provides recommendations for future research opportunities. The recommendations are suggested based on the observations, findings, and analysis of the current study (Figure 6.1).

6.1 Limitations of Current Study

6.1.1 Ranges of Independent Variables

The compressive stress of freshwater ice near the melting point ranges from 1.0 - 10.0 MPa over a strain rate range of 0.5-75 s⁻¹ (Qi et al., 2017). As the experiment was conducted at -1°C with freshwater ice, the contact pressure was in the range 112-826 kPa. Considering the compressive strength of ice, the contact pressure range was not beyond 1000kPa. The compressive strength of the ice sample was not measured in this study. For more accurate understanding of the importance of ice strength, the compressive strength of the ice could be measured, and the contact pressure range should be selected accordingly.

The duration of applied pressure ranged from 1-120 minutes as the cold room temperature could not be maintained continuously beyond 6 hours. This is a realistic range as it is likely that significant abrasion would only be generated where bonding-breaking occurred at relatively high frequency. However it would be useful to extend the range of bonding time to cover the range of tidal cycles and possibly up to a full day cycle of 24 hours.

6.1.2 Controlled Environment and Equipment

The temperature of the cold room could not be controlled very accurately. Future experiments should be conducted under a more controlled environment.

The lever arm apparatus was operated using a hand drill. The adhesion strength of ice depends on the loading rate. Though this equipment is easy to carry and has an approximately constant velocity, a more precise motorized instrument could be used for better control of the applied

bond breaking force.

6.1.3 Surface Roughness Measurement and Microscopic Analysis

The experiment was conducted in a smaller scale. Thus a minimal amount of concrete abrasion was observed, even after a series of experiments. The erosion of the concrete surface was also nominal and only observed after multiple numbers of experiments. As the ice adhesion largely depends on the surface roughness, the surface profile of the concrete specimens needs to be measured, ideally after each trial. Also, the concrete surface could be compared on a microscopic scale - before and after each experiment.

Although photographs were taken and the weight of the concrete specimens was measured before, and after each experiment, the exact amount of abrasion was not possible to collect due to the minimal amount. Thus the experiment scale needs to be significant, and the abraded particles need to be measured separately after each experiment.

6.1.4 Compressive test of Rock Samples

The aggregate samples were used to measure the adfreeze bond strength between the ice and the aggregate. The samples were ordered from the aggregate manufacturing company . Due to the lack of rock specimens, a compressive test of the rock samples was not possible.

The surface roughness and microscopic analysis of the rock sample needs to be done as the adfreeze bond highly depends on the surface roughness and microscopic pores of materials.

6.2 Recommendation for Future Research

6.2.1 Items that could not be completed

It is noted that some aspects of this program were interrupted by the occurrence of the Pandemic in early 2020 and the subsequent closure of the University and Laboratories. These aspects of this study could be taken on as a future research project as operations return to

normality. In addition to these aspects, some further suggestions for expanding the research are noted in the following section.

6.2.2 Inclusion of Other Independent Variables

The current experiment was conducted under two independent variables- contact pressure and time. From the current experimental findings, it was observed that the ice concrete adhesion may also be dependent on the temperature. The change in ice concrete interface can be obtained under different temperature using the same test matrix.

The current experiment was conducted using concrete samples with a fixed contact area. As prior studies have shown (Saeki, 2011) that the contact area has an effect on the adhesion strength, the size of concrete samples, or contact area, can be introduced as another variable.

The adfreeze bond strength also depends on the loading rate, thus the adhesion strength can be obtained with same contact duration and applied pressure under different loading rates.

6.2.3 Variation of Concrete Mix Design

This study has observed that the individual components of concrete have different adhesion strength with ice. Further studies can be developed using different concrete mix designs with different aggregates such as lightweight aggregates to observe the adhesion bond strength and corresponding abrasion. The adhesion was observed to be directly proportional to the contact pressure. Thus a lightweight aggregate with lower contact pressure may have a lower adhesion bond strength with ice.

There was no direct relation found between ice-concrete adhesion strength and concrete abrasion. Thus the adhesion bond strength between ice concrete interfaces may not be directly proportional to the concrete abrasion. Hence the concrete abrasion may depend more strongly on the material properties and surface properties of the concrete sample

6.2.4 Full Scale and Long term Experiment

The current data set and experimental study has given some ideas about the adhesion strength of ice at laboratory scale. An experiment could be designed at full scale to obtain further data. Also a long term experiment can be designed for current concrete structures over a wide region. Structural damage can be observed during a long duration of time, with data will collected and analyzed to observe abrasion effects on concrete. As part of such an experiment a method of observing the extent and strength of adhesion would need to be developed and incorporated into the testing or observation.

6.2.5 Statistical Analysis

An experiment can be designed using DOE software for a more rigorous statistical analysis. This statistical analysis will help to obtain the impact of independent variables and the statistical significance of the collected data set. A mathematical model can be constructed using a larger set of data with multiple replications to theoretically calculate the adhesion strength of ice and concrete for a wider range of applied pressure and duration. This analysis will help to develop calculation methods for ice adhesion strength in a large scale. Including the surface roughness of different construction materials in the statistical model can also give a foresight for the adhesion strength and abrasion mechanism. Although ice adhesion is a well known problem for colder region structures, the adhesion strength and abrasion depends on multiple parameters. These parameters are easily influenced by different factors, such as geographic location, climate and type of ice. Developing a statistical model with various independent variables will help to create a method for calculating adhesion strength and abrasion mechanisms for a wide range of cold region constructions.

The data from this experiment could also be treated differently by including all measurements in the statistical analysis, rather than first averaging the replications. This would allow the variability in the experimental measurements to be included in the analysis.

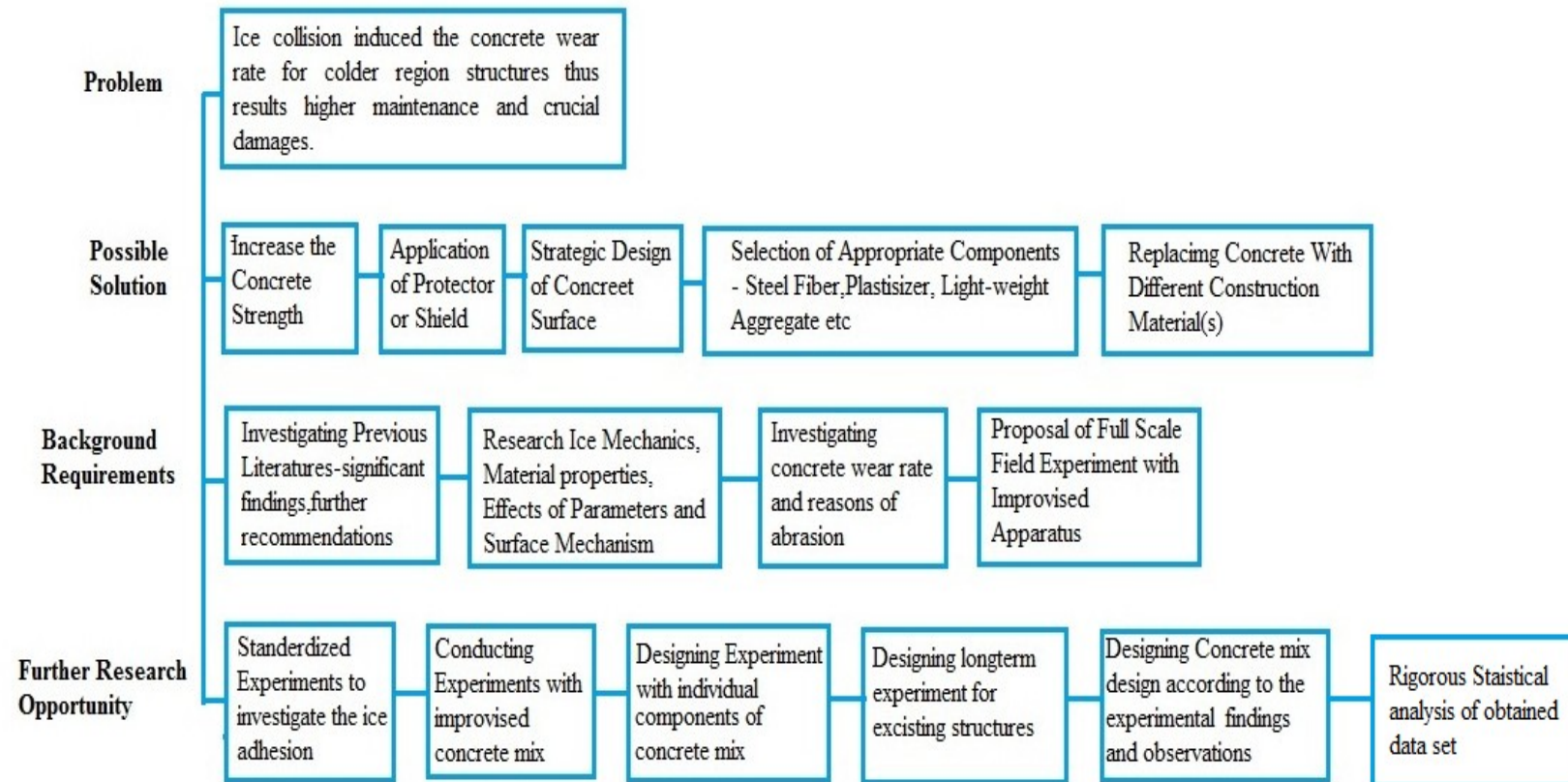


Figure 6.1: Research Objective and Future Opportunities

References

- Amanda Ryan, B., & John, S. (2018). *ICE WEAR AND ABRASION OF MARINE CONCRETE: Design of Experimental Apparatus and Procedures*. March.
- B. C. Gerwick, J. A. D. B. (n.d.). Thermal and Durability Considerations for Composite Steel/Concrete Sandwich Structures. *ACI Symposium Publication*, 109. <https://doi.org/10.14359/2804>
- Baddeley, A. (2020). *Chapter 6 : Chapter 6 Instructions*. 6, 5–6.
- Barker, A., Bruneau, S., & Colbourne, B. (2019). Adhesion of ice to concrete: Bonds and their influence on abrasion mechanisms. *Proceedings of the International Conference on Port and Ocean Engineering under Arctic Conditions, POAC, 2019-June(1987)*.
- Bekker, A. T., Uvarova, T. E., Pomnikov, E. E., Farafonov, A. E., Prytkov, I. G., & Tyutrin, R. S. (2011). Experimental study of concrete resistance to ice abrasion. *Proceedings of the International Offshore and Polar Engineering Conference, January*, 1044–1047.
- Bruneau, S. E., Dillenburg, A. K., & Ritter, S. (2013). Ice sample production techniques and indentation tests for laboratory experiments simulating ship collisions with ice. *Proceedings of the International Offshore and Polar Engineering Conference*, 1268–1271.
- Christensen, F. T. (1987). Vertical ice forces on long straight walls. *Cold Regions Science and Technology*, 13(3), 215–218. [https://doi.org/10.1016/0165-232X\(87\)90001-2](https://doi.org/10.1016/0165-232X(87)90001-2)
- Fiorio, B. (2005). Wear characterisation and degradation mechanisms of a concrete surface under ice friction. *Construction and Building Materials*, 19(5), 366–375. <https://doi.org/10.1016/j.conbuildmat.2004.07.020>
- Fiorio, B., Meyssonnier, J., & Boulon, M. (2002). Experimental study of the friction of ice over concrete under simplified ice-structure interaction conditions. *Canadian Journal of Civil Engineering*, 29(3), 347–359. <https://doi.org/10.1139/102-012>
- Greaker, N. . (2014). *Greaker, N.S. Laboratory Measurements of Ice-Concrete Abrasion with Different Types of Ice Quality* [(Master's thesis, Institutt for bygg, anlegg og transport)]. <http://hdl.handle.net/11250/233032>
- Gu, J., Wu, X., Cuypers, H., & Wastiels, J. (1998). *Transactions on Engineering Sciences vol 21*, © 1998 WIT Press, www.witpress.com, ISSN 1743-3533. 17, 589–598.
- Huovinen, S. (1990). Abrasion of concrete by ice in arctic sea structures. *Publications - Technical Research Centre of Finland*, 62.
- ICE-STRUCTURE INTERACTION Devinder S . Sodhi. (n.d.). *Engineering*.
- Itoh, Y., Yoshida, A., Tsuchiya, M., Katoh, K., Sasaki, K., & Saeki, H. (1988). An experimental study on abrasion of concrete due to sea ice. In: *Otc 88 Proc., Twentieth Annual Offshore Technol. Conf., (Houston, U.S.a.: May 2-5, 1988)*, 2, Richar, 61–68.

<https://doi.org/10.4043/5687-ms>

- Itoh, Yoshishige, Tanaka, Y., & Saeki, H. (1994). Estimation Method For Abrasion of Concrete Structures Due to Sea Ice Movement. In *The Fourth International Offshore and Polar Engineering Conference* (p. 8). International Society of Offshore and Polar Engineers. <https://doi.org/>
- Jacobsen, S., Scherer, G. W., & Schulson, E. M. (2015). Concrete-ice abrasion mechanics. *Cement and Concrete Research*, *73*, 79–95. <https://doi.org/10.1016/j.cemconres.2015.01.001>
- Makkonen, L. (2012). Ice adhesion - Theory, measurements and countermeasures. *Journal of Adhesion Science and Technology*, *26*(4–5), 413–445. <https://doi.org/10.1163/016942411X574583>
- Møen, E., Høiseith, K. V., Leira, B., & Høyland, K. V. (2015). Experimental study of concrete abrasion due to ice friction — Part I: Set-up, ice abrasion vs. material properties and exposure conditions. *Cold Regions Science and Technology*, *110*, 183–201. <https://doi.org/https://doi.org/10.1016/j.coldregions.2014.09.008>
- Møen, E., Jacobsen, S., & Myhra, H. A. (2008). Ice Abrasion Data on Concrete Structures - Overview. *Nordic Concrete Federation Workshop Proceedings*, 59–103.
- Murase, H., & Nanishi, K. (1985). On the Relationship of Thermodynamic and Physical Properties of Polymers With Ice Adhesion. *Annals of Glaciology*, *6*, 146–149. <https://doi.org/10.3189/1985aog6-1-146-149>
- Nakazawa, N., Saeki, H., Ono, T., Takeuchi, T., & Kanie, S. (1988). Ice Forces due to Changes in Water Level and Adfreeze Bond Strength Between Sea Ice and Various Materials. *Journal of Offshore Mechanics and Arctic Engineering*, *110*(1), 74–80. <https://doi.org/10.1115/1.3257127>
- Nevel, D. E. (1980). Bending and Buckling of a Wedge on an Elastic Foundation. *Physics and Mechanics of Ice*, 278–288. https://doi.org/10.1007/978-3-642-81434-1_20
- Oksanen, P. (1980). *Coefficient of friction between ice and some construction materials, plastics and coatings*. VTT Technical Research Centre of Finland. Valtion teknillinen tutkimuskeskus: Rakennetekniikan laboratorio. Tiedonanto No.
- Qi, C., Lian, J., Ouyang, Q., & Zhao, X. (2017). Dynamic compressive strength and failure of natural lake ice under moderate strain rates at near melting point temperature. *Latin American Journal of Solids and Structures*, *14*(9), 1669–1694. <https://doi.org/10.1590/1679-78253907>
- Saeki, H., Ono, T., Nakazawa, N., Sakai, M., & Tanaka, S. (1984). The coefficient of friction between sea ice and various materials used in offshore structure. *Proceedings of the Annual Offshore Technology Conference, 1984-May*(March 1986), 375–382. <https://doi.org/10.4043/4689-ms>
- Saeki, Hiroshi. (2011). Mechanical properties between ice and various materials used in

hydraulic structures: The Jin S. Chung award lecture, 2010. *International Journal of Offshore and Polar Engineering*, 21(2), 81–90.

Saeki, Hiroshi, Ono, T., Zong, N. E., & Nakazawa, N. (1985). Experimental Study on Direct Shear Strength of Sea Ice. *Annals of Glaciology*, 6, 218–221. <https://doi.org/10.3189/1985aog6-1-218-221>

Shamsutdinova, G. R., Hendriks, M. A. N., & Jacobsen, S. (n.d.). *CONCRETE-ICE ABRASION: SURFACE ROUGHNESS*.

Terahima, T., Nakazawa, N., Kioka, S., Usami, N., & Saeki, H. (2006). Vertical ice forces on pile structures under water level changes. *Proceedings Oh the 18th IAHR International Symposium on Ice (2006)*, 145–152.

Tijssen, J., Bruneau, S., & Colbourne, B. (2015). Laboratory examination of ice loads and effects on concrete surfaces from bi-axial collision and adhesion events. *Proceedings of the International Conference on Port and Ocean Engineering under Arctic Conditions, POAC, 2015-Janua*.